Computers and Fluids 274 (2024) 106233

Contents lists available at ScienceDirect

Computers and Fluids

journal homepage: www.elsevier.com/locate/compfluid

Modified variational iteration method and its convergence analysis for solving nonlinear aggregation population balance equation

Sonia Yadav [a,1], Mehakpreet Singh [b,*,1], Sukhjit Singh [a], Stefan Heinrich [c], Jitendra Kumar [d]

[a] Department of Mathematics and computing, Dr. B.R. Ambedkar National Institute of Technology Jalandhar, Punjab, India
[b] Mathematics Applications Consortium for Science and Industry (MACSI), Department of Mathematics and Statistics, University of Limerick, Limerick V94 T9PX, Ireland
[c] Institute of Solids Process Engineering and Particle Technology, Hamburg University of Technology, Denickestraße 15, 21073, Hamburg, Germany
[d] Department of Mathematics, Indian Institute of Technology Ropar, Punjab 140001, India

ARTICLE INFO

MSC:
primary 34A12
35Q70
45K05
secondary 47J35

Keywords:
Nonlinear aggregation equation
Variational iteration method
Contraction mapping principle
Lagrange multiplier
Convergence analysis

ABSTRACT

This study proposes a novel approach based on the variational iteration method to solve the nonlinear aggregation population balance equation. The approach provides great flexibility by allowing the selection of appropriate linear operators and efficiently determining the Lagrange multiplier in the nonlinear aggregation population balance equation. The mathematical derivation is supported by conducting a detailed convergence analysis using the contraction mapping principle in the Banach space. Furthermore, error estimates for the approximate solutions are derived, thereby improving our understanding of the accuracy and reliability of the proposed method. To validate the new approach, the obtained solutions are compared with the exact solutions for analytically tractable kernels. However, for more complex physically relevant kernels including polymerization, Ruckenstein/Pulvermacher, and bilinear kernels, due to lack exact solutions, the obtained series solutions corresponding to different initial conditions are verified against the finite volume scheme (kumar et al., 2016). The outcomes illustrate that the proposed approach offers superior approximations of number density functions with fewer terms and demonstrates higher accuracy over extended time domains than the traditional variational iterative method. The new approach also has the tendency to capture the zeroth and first order moments of the number density function with high precision.

1. Introduction

In recent decades, numerous real-life applications have encompassed a wide range of phenomena including the precipitation, formation of raindrops, planetesimal formation, crystallization, granulation, and coagulation of red blood cells [1–5] is of great industrial and academic interest. The dynamics of particles are effectively described using the population balance equation [6–8], which utilizes number density functions to quantify the distribution of particles based on their volumes (sizes) within the entire population. The number density functions play a crucial role in providing a comprehensive representation of the particle population. They offer a detailed analysis of the behaviour and evolution of particles over time. By characterizing the distribution of particles based on their volumes, the number density function provides a thorough examination of how the population grow or diminish over time. This information is invaluable for understanding the underlying dynamics, particle interactions, and predictions about the future behaviour of the particulate system.

The primary objective of the present study is to observe the behaviour of particles within a system experiencing property changes as a result of the aggregation process. Aggregation refers to the merging of two or more particles resulting in the formation of a larger particle. The continuous aggregation population balance equation (APBE) is mathematically represented by a nonlinear integro-partial differential equation [9,10] given by

$$\frac{\partial y(p,t)}{\partial t} = \mathcal{R}_{\mathbf{agg}}(y)(p,t) := \mathcal{R}_{\mathbf{source}}(y)(p,t) - \mathcal{R}_{\mathbf{sink}}(y)(p,t), \qquad p \in [0,\infty), t \in [0,T] \tag{1}$$

* Corresponding author.
E-mail addresses: Mehakpreet.Singh@ul.ie (M. Singh), kundalss@nitj.ac.in (S. Singh), jkumar@iitrpr.ac.in (J. Kumar).
[1] Both authors contributed equally.

https://doi.org/10.1016/j.compfluid.2024.106233
Received 18 August 2023; Received in revised form 1 February 2024; Accepted 28 February 2024
Available online 5 March 2024

with an initial condition

$$y(p,0) = y_0(p) \geq 0, \tag{2}$$

and the aggregation source and sink terms are

$$\mathcal{R}_{\text{source}}(y)(p,t) = \frac{1}{2}\int_0^p l(p-q,q)y(p-q,t)y(q,t)dq,$$

$$\mathcal{R}_{\text{sink}}(y)(p,t) = \int_0^\infty l(p,q)y(p,t)y(q,t)dq.$$

Here, $y(p,t)$ represents the number density distribution of the particles having particle property p at time t. The source term in the equation accounts for the birth of new particles with property p through the merging of particles with properties $p-q$ and q. On the other hand, the sink term represents the death of particles with property p as a result of their aggregation with particles possessing property q. The merging process is influenced by the aggregation kernel $l(p,q)$, which determines the rate at which p and q particles combine to form particle of property $p+q$. It is non negative and symmetric in nature. The aggregation process leads to a decrease in the overall number of particles while maintaining a constant mass or volume within the system.

Smoluchowski was the first who established this equation and formulated its solution for the constant aggregation kernel [11]. For the empirical constant ($l(p,q) = 1$), sum ($l(p,q) = p+q$) and product ($l(p,q) = pq$) kernels, the analytical solutions exist in the literature (refer to [12–14] and references therein). However, obtaining exact solutions for physically relevant kernels such as polymerization, Ruckenstein/Pulvermacher, and Bilinear kernels in terms of number density functions remains a challenging and computationally expensive task. Some numerical approaches are also available for tackling problems related to complex physically relevant kernels [15–25]. Although numerical approaches are useful for solving these problems, they have restrictions due to the discretization or linearization of parameters such as grid size and time step that might change the physical behaviour of the problem. Some other relevant methods available in the literature for similar type of nonlinear partial differential equation or fraction differential equation including generalized shallow water wave equation, fractional zoomeron equation, and Zakhrov-Kuznetsov equation can be found here [26–32].

Among several classes of methods, the semi-analytical approaches are free from many traits including mesh discretization, linearization, and sets of basis functions. Several semi-analytical approaches have been utilized to construct series approximation solutions for the aggregation problem in the past decade. Biazar et al. [33] obtained the series solution of (1) for the constant ($l(p,q) = 1$) and product ($l(p,q) = pq$) kernel by using Homotopy perturbation method (HPM). Later, Singh et al. [34] established the solution of a aggregation Eq. (1) using the Adomian decomposition method (ADM) for the constant, product and sum ($l(p,q) = p+q$) kernel. Moreover, Hasseinea et al. [35] conducted a comparative study among variational iteration method (VIM), HPM and ADM for the product kernel and demonstrated that variational iteration and HPM are more efficient approaches and do not require the calculation of the Adomian polynomials (typically involve complicated algebraic calculations). Kaur et al. [13] developed the Homotopy perturbation method for approximating the solution of Eq. (1) for the constant, sum, product and Ruckenstein/Pulvermacher kernel ($l(p,q) = p^{2/3} + q^{2/3}$). Recently, Yadav et al. [36] addressed the missing convergence analysis of the homotopy analysis method (HAM) for solving pure aggregation and pure fragmentation population balance equations and further extended the method to determine the series solutions for a simultaneous aggregation-fragmentation (SAF) population balance equation. In [37], authors implemented the optimized decomposition method to obtain the series solution and showed better accuracy than the ADM. Recently, Arora et al. [38] examined the variational iteration method and optimal variational iterative method to solve the aggregation Eq. (1) in the series form. It was shown that while the accuracy improves to some extent using the optimal variational iterative method but computing higher order terms of the truncated series consumes enormous CPU time. Moreover, the optimal variational iterative method includes a convergence control parameter computed by minimizing the residual error, which requires a large computational time as mentioned in [38].

One significant drawback of the existing semi-analytical approaches is their limited applicability to shorter time domains. As the time domain extends, the accuracy of the obtained solutions deteriorates significantly, imposing restrictions on their practical applications. This limitation stems from the inherent complexity of the underlying equations and the approximations made during the solution process. Consequently, these semi-analytical approaches may not be suitable for studying long-term dynamics or processes that evolve over extended periods. Over the past few decades, various modifications to VIM have been made including the hybrid spectral-variational iteration method for solving nonlinear equations arising in heat transfer [39], an improved piecewise variational iteration approach for strongly nonlinear oscillators [40], and a piecewise spectral-variational iteration method to solve astrophysical equations [41]. Soltani et al. [42] extended the traditional VIM and demonstrated substantial improvement over the traditional VIM.

The goal of this study is to find the novel series solutions of the nonlinear aggregation equation using the modified variational iteration method (MVIM). The MVIM offers tremendous flexibility in selecting linear operators for nonlinear equations and effectively identifies the Lagrange multiplier. The testing of the new approach is done for both analytically tractable and physically relevant kernels. It will be shown that irrespective of the complexity of the aggregation kernels, the proposed approach requires only a few series terms to capture the number density functions over extended time and shows superior results than the traditional VIM. In addition, the proposed approach has the tendency to track integral properties including zeroth and first order moments of the number density function with high precision.

The rest of the paper is organized as follows: we introduce the general methodologies of both VIM and MVIM along with the implementation of these approaches on the nonlinear aggregation equation and obtain their Lagrange multiplier in Section 2. In Section 3, the convergence of the MVIM for the aggregation equation is discussed in detail using the principle of contraction mapping. In Section 4, the testing of the MVIM is done to demonstrate the advantages of employing the MVIM over the existing VIM. Finally, some concluding remarks and discussion will be done in the last Section 5.

2. Semi analytical methods

This section is devoted to provide the mathematical formulations of both VIM and MVIM to approximate a nonlinear APBE (1). Before deriving these, let us first discuss the fundamental principles of the VIM and MVIM for solving partial differential equations.

2.1. Basic idea of VIM

Ji-Haun He [43] introduced a reliable and efficient VIM to tackle linear and nonlinear differential equations. Unlike standard numerical approaches, VIM does not require any linearization, transformation, discretization, or perturbation. The concept of VIM is based on generating a correction functional using a general Lagrange multiplier, and the multiplier's value is chosen in such a way that its correction solution improves the successive approximation. Now, to comprehend the basic idea of VIM, we consider the general partial differential equation of the following form

$$\mathcal{L}[y(p,t)] + \mathcal{N}[y(p,t)] = h(p,t) \qquad \text{with} \qquad y(p,0) = g(p), \tag{3}$$

is considered. Here $\mathcal{L}$ and $\mathcal{N}$ are the linear and nonlinear operators, respectively and $g(p)$ is the known continuous function. Using the VIM, the correction functional iteration is written as

$$y_{k+1}(p,t) = y_k(p,t) + \int_0^t \lambda(\eta,t)[\mathcal{L}[y_k(p,\eta)] + \mathcal{N}[\tilde{y}_k(p,\eta)] - h(p,\eta)]d\eta. \tag{4}$$

To find the optimal value of the general Lagrange multiplier $\lambda(\eta,t)$, the restricted variation for nonlinear terms is considered, i.e., $\delta\mathcal{N}[\tilde{y}_k] = 0$. Now, by assuming any selecting function that satisfies the initial condition and the Lagrange multiplier, it will be simple to obtain the subsequent approximations $y_k(p,t)$ of the solution $y(p,t)$. Furthermore, the exact solution may be found as

$$y(p,t) = \lim_{k\to\infty} y_k(p,t). \tag{5}$$

2.1.1. VIM for aggregation equation

In this subsection, the mathematical formulation of the recently developed VIM [38] to solve an APBE (1) is provided. For deriving the expression of VIM, the aggregation Eq. (1) can be rewritten in the following form:

$$\mathcal{L}[y(p,t)] + \mathcal{N}[y(p,t)] = 0, \tag{6}$$

where,

$$\mathcal{L}[y] = \frac{\partial y}{\partial t},$$

and

$$\mathcal{N}[y] = -\frac{1}{2}\int_0^p k(p-q,q)y(p-q,t)y(q,t)dq + \int_0^\infty k(p,q)y(p,t)y(q,t)dq,$$

subject to an initial condition $y(p,0) = g(p)$. According to VIM, the correction functional can be constructed in the form

$$y_{k+1}(p,t) = y_k(p,t) + \int_0^t \lambda(\eta,t)\left[\frac{\partial y_k(p,\eta)}{\partial\eta} - \frac{1}{2}\int_0^p l(p-q,q)\tilde{y}_k(p-q,\eta)\tilde{y}_k(q,\eta)dq + \int_0^\infty l(p,q)\tilde{y}_k(p,\eta)\tilde{y}_k(q,\eta)dq\right]d\eta, \tag{7}$$

where $\tilde{y}$ is considered the restricted variation, that is, $\delta(\tilde{y}) = 0$. The optimal value of $\lambda(\eta,t)$ is identified via variational theory. Now, calculate variation with respect to y_n and we have the following stationary conditions $\lambda'(\eta,t) = 0$ and $1 + \lambda(\eta,t)|_{\eta=t} = 0$ which yields $\lambda(\eta,t) = -1$. The following iteration formula is obtained for VIM by substituting the identified multiplier into Eq. (7) as

$$y_{k+1}(p,t) = y_k(p,t) - \int_0^t \left[\frac{\partial y_k(p,\eta)}{\partial\eta} - \frac{1}{2}\int_0^p l(p-q,q)y_k(p-q,\eta)y_k(q,\eta)dq + \int_0^\infty l(p,q)y_k(p,\eta)y_k(q,\eta)dq\right]d\eta. \tag{8}$$

2.2. Basic idea of modified VIM

VIM has been intensively used to handle nonlinear problems, however, accuracy for a certain class of problems is always questionable. Here we are adapting a MVIM [42] for solving a nonlinear APBE. This modified approach aims to tackle the limitations encountered in traditional VIM when solving a nonlinear APBE. According to this, Eq. (3) can be rewritten as follows [44–47]:

$$\mathcal{L}[y(p,t)] + \overbrace{\mathcal{L}^*[y(p,t)] - \mathcal{L}^*[y(p,t)]} + \mathcal{N}[y(p,t)] = h(p,t), \tag{9}$$

where $\mathcal{L}^*[y(p,t)]$ denotes an arbitrary linear operator. Now, we can build a correction functional using $\mathcal{L}[y(p,t)] + \mathcal{L}^*[y(p,t)]$ as a linear operator in the following form

$$y_{k+1}(p,t) = y_k(p,t) + \int_0^t \lambda(\eta,t)[\mathcal{L}[y_k(p,\eta)] + \mathcal{L}^*[y_k(p,\eta)] - \mathcal{L}^*[\tilde{y}_k(p,\eta)] + \mathcal{N}[\tilde{y}_k(p,\eta)] - h(p,\eta)]d\eta. \tag{10}$$

Again, we consider the restricted variation for the nonlinear term, that is, $\delta\mathcal{N}[\tilde{y}_k] = 0$, $\delta\mathcal{L}^*[\tilde{y}_k] = 0$ and obtain the optimal value of the Lagrange multiplier, which is differs from the previous one. In addition, we can choose an arbitrary linear operator that allows us to identify the effective Lagrange multiplier.

2.2.1. MVIM for nonlinear aggregation equation

Now, let us derive the mathematical expression for the MVIM to approximate the solution of an aggregation Eq. (1). For the mathematical expression of MVIM, assume $(\mathcal{L}+I)$ as a linear operator and $(\mathcal{N}-I)$ as a nonlinear operator. Thus, the correction functional can be constructed in the form

$$y_{k+1}(p,t) = y_k(p,t) + \int_0^t \lambda(\eta,t)\left[\frac{\partial y_k(p,\eta)}{\partial \eta} + y_k(p,\eta) - \frac{1}{2}\int_0^p l(p-q,q)\tilde{y}_k(p-q,\eta)\tilde{y}_k(q,\eta)dq + \int_0^\infty l(p,q)\tilde{y}_k(p,\eta)\tilde{y}_k(q,\eta)dq - \tilde{y}_k(p,\eta)\right]d\eta. \tag{11}$$

Again, $\tilde{y}$ is considered the restricted variation i.e. $\delta(\tilde{y}) = 0$. Taking variation with respect to y_k and we get the following stationary conditions

$$\begin{cases} 1 + \lambda(\eta,t)|_{\eta=t} = 0, \\ \lambda'(\eta,t) - \lambda(\eta,t) = 0. \end{cases}$$

Thus, the Lagrange multiplier can be identified as $\lambda(\eta,t) = -e^{\eta-t}$. Now, by substituting the value of $\lambda(\eta,t)$ in (11), we have obtained the iterative formula for MVIM given by

$$y_{k+1}(p,t) = y_k(p,t) - \int_0^t e^{\eta-t}\left[\frac{\partial y_k(p,\eta)}{\partial \eta} - \frac{1}{2}\int_0^p l(p-q,q)y_k(p-q,\eta)y_k(q,\eta)dq + \int_0^\infty l(p,q)y_k(p,\eta)y_k(q,\eta)dq\right]d\eta. \tag{12}$$

We can use $y_0 = g(p)$ as the initial approximation to solve iteratively Eqs. (8) and (12). The exact solution may be obtained by using

$$y(p,t) = \lim_{k\to\infty} y_k(p,t). \tag{13}$$

3. Convergence analysis

In this section, the fixed point theorem is used to establish the sufficient conditions for the convergence of sequence defined in (12) and the maximum absolute error of the sequence is also estimated.

Consider the Banach space $\mathbb{J} = (C([0,T] : L^1[0,\infty), \|.\|)$ with the norm

$$\|y\| = \sup_{t\in[0,T]}\int_0^\infty |y(p,t)|dp, \tag{14}$$

and define the operator $\mathcal{M} : \mathbb{J} \to \mathbb{J}$ as

$$\mathcal{M}[y] = -\int_0^t e^{\eta-t}\left[\frac{\partial y(p,\eta)}{\partial \eta} - \frac{1}{2}\int_0^p l(p-q,q)y(p-q,\eta)y(q,\eta)dq + \int_0^\infty l(p,q)y(p,\eta)y(q,\eta)dq\right]d\eta. \tag{15}$$

The components y_k and z_k, for $k = 0, 1$ are given by

$$\begin{cases} z_0(p) = y_0(p), \\ \mathcal{A}_0(p) = z_0(p), \end{cases}$$

and

$$\begin{cases} z_1(p,t) = \mathcal{M}[z_0], \\ \mathcal{A}_1(p,t) = z_0(p) + z_1(p,t). \end{cases}$$

In general, for $k \geq 2$, we have

$$\begin{cases} z_k(p,t) = \mathcal{M}[z_0 + z_1 + z_2 + \ldots + z_{k-1}], \\ \mathcal{A}_k(p,t) = z_0(p) + z_1(p,t) + \ldots + z_k(p,t). \end{cases} \tag{16}$$

Therefore, as a result, we have $y(p,t) = \lim_{k\to\infty} y_k(p,t) = \sum_{k=0}^\infty z_k$. If the initial condition is satisfied, we can freely choose $z_0 = y_0$. The proper choice of the initial approximation z_0 is essential to the method's effectiveness. With the help of nth order truncated series $\sum_{k=0}^n z_k$, we can approximate the solution $y(p,t) = \sum_{k=0}^\infty z_k$.

Theorem 3.1. *Let $\mathcal{M} : \mathbb{J} \to \mathbb{J}$ be an operator defined over $\mathbb{J}$. The series solution $y(p,t) = \sum_{k=0}^\infty z_k$ converges if there exists $0 < \varphi < 1$, such that $\|\mathcal{M}[z_0 + z_1 + z_2 + \cdots + z_k]\| \leq \varphi\|\mathcal{M}[z_0 + z_1 + z_2 + \cdots + z_{k-1}]\|$, that is, $\beta_k \leq \varphi$ for all $k \in \mathbb{N}\cup\{0\}$ where $\beta_k = \begin{cases} \frac{\|z_{k+1}\|}{\|z_k\|}, & \|z_k\| \neq 0 \\ 0, & \|z_k\| = 0. \end{cases}$*

Proof. First, we have to show $\{\mathcal{A}_k\}_{k=0}^\infty$ is Cauchy sequence. For this reason, we consider

$$\|\mathcal{A}_{k+1} - \mathcal{A}_k\| = \|z_{k+1}\| \leq \varphi\|z_k\| \leq \varphi^2\|z_{k-1}\| \leq \cdots \leq \varphi^{k+1}\|z_0\|.$$

Now, $\forall\ k \geq m$, we have

$$\begin{aligned}\|\mathcal{A}_k - \mathcal{A}_m\| &= \|(\mathcal{A}_k - \mathcal{A}_{k-1}) + (\mathcal{A}_{k-1} - \mathcal{A}_{k-2}) + \cdots + (\mathcal{A}_{m+1} - \mathcal{A}_m)\| \\ &\leq \|\mathcal{A}_k - \mathcal{A}_{k-1}\| + \|\mathcal{A}_{k-1} - \mathcal{A}_{k-2}\| + \cdots + \|\mathcal{A}_{m+1} - \mathcal{A}_m\| \\ &\leq \varphi^k\|z_0\| + \varphi^{k-1}\|z_0\| + \ldots + \varphi^{m+1}\|z_0\| \\ &= \frac{1-\varphi^{k-m}}{1-\varphi}\varphi^{m+1}\|z_0\|. \end{aligned} \tag{17}$$

Thus, $\lim_{m\to\infty}\|\mathcal{A}_k - \mathcal{A}_m\| = 0$, since $0 < \varphi < 1$. As a result, the sequence $\{\mathcal{A}_k\}_{k-0}^{\infty}$ is Cauchy in Banach space, hence $y(p,t) = \sum_{k=0}^{\infty} z_k$ converges. □

Theorem 3.2. *Consider $\mathcal{L}_1 \equiv (\mathcal{L} + I)$ as linear operator and $\mathcal{N}_1 \equiv (\mathcal{N} - I)$ as a nonlinear operator for MVIM and $y(p,t) = \sum_{k=0}^{\infty} z_k$, then $y(p,t)$ is the exact solution of the nonlinear aggregation Eq. (6). In addition, if the approximated solution of Eq. (6) is given by the truncated series $\sum_{k=0}^{m} z_k(p,t)$, then the maximum error $\mathcal{E}_m$ is determined as*

$$\mathcal{E}_m \leq \frac{1}{1-\varphi}\varphi^{m+1}\|z_0\|. \tag{18}$$

Proof. If the series solution $\sum_{k=0}^{\infty} z_k(p,t)$ converges then, we get $\lim_{k\to\infty} z_k = 0$. Also, $\sum_{k=0}^{m}[z_{k+1} - z_k] = z_{m+1} - z_0$.

Thus, we have $\sum_{k=0}^{\infty}[z_{k+1} - z_k] = \lim_{m\to\infty} z_{m+1} - z_0 = -z_0$.

Now, by applying the linear operator $\mathcal{L}_1$ on both side, we get

$$\sum_{k=0}^{\infty}\mathcal{L}_1[z_{k+1} - z_k] = -\mathcal{L}_1[z_0] = -\left[\frac{\partial}{\partial t} + I\right]z_0 = -z_0. \tag{19}$$

Eq. (15) can be written as

$$\begin{aligned}\mathcal{M}[y] = -\int_0^t e^{\eta-t}\Bigg[\frac{\partial y(p,\eta)}{\partial\eta} + y(p,\eta) - \frac{1}{2}\int_0^p l(p-q,q)y(p-q,\eta)y(q,\eta)dq \\ + \int_0^{\infty} l(p,q)y(p,\eta)y(q,\eta)dq - y(p,\eta)\Bigg]d\eta = -\int_0^t e^{\eta-t}[\mathcal{L}_1(y) + \mathcal{N}_1(y)]d\eta. \end{aligned} \tag{20}$$

Now, from definition (16) and (20), we get

$$\begin{aligned}\mathcal{L}_1[z_{k+1} - z_k] &= \mathcal{L}_1[\mathcal{M}[z_0 + z_1 + \cdot + z_k] - \mathcal{M}[z_0 + z_1 + \cdots + z_{k-1}]] \\ &= \mathcal{L}_1\left[-\int_0^t e^{\eta-t}[\mathcal{L}_1(z_0 + z_1 + \cdots + z_k) + \mathcal{N}_1(z_0 + z_1 + \cdots + z_k)]d\eta + \int_0^t e^{\eta-t}[\mathcal{L}_1(z_0 + z_1 + \cdots + z_{k-1}) + \mathcal{N}_1(z_0 + z_1 + \cdots + z_{k-1})]d\eta\right] \\ &= \mathcal{L}_1\left[-\int_0^t e^{\eta-t}[\mathcal{L}_1(z_k) + \mathcal{N}_1(z_0 + z_1 + \cdots + z_k) - \mathcal{N}_1(z_0 + z_1 + \cdots + z_{k-1})]d\eta\right]. \end{aligned}$$

By substituting the value of operator $\mathcal{L}_1 \equiv \left(\frac{\partial}{\partial t} + I\right)$, we have

$$\begin{cases}\mathcal{L}_1[z_1 - z_0] = -\{\mathcal{N}_1(z_0) + 2z_0\}, \\ \mathcal{L}_1[z_{k+1} - z_k] = -\{\mathcal{L}_1(z_k) + \mathcal{N}_1(z_0 + z_1 + \cdots + z_k) - \mathcal{N}_1(z_0 + z_1 + \cdots + z_{k-1})\} \quad \text{for } k \geq 1. \end{cases}$$

As a result, we have

$$\begin{aligned}\sum_{k=0}^{m}\mathcal{L}_1[z_{k+1} - z_k] = -\big\{&\mathcal{N}_1(z_0) + 2z_0 \\ &+ \mathcal{L}_1(z_1) + \mathcal{N}_1(z_0 + z_1) - \mathcal{N}_1(z_0) \\ &\vdots \\ &+ \mathcal{L}_1(z_{m-1}) + \mathcal{N}_1(z_0 + z_1 + \cdots + z_{m-1}) - \mathcal{N}_1(z_0 + z_1 + \cdots + z_{m-2}) \\ &+ \mathcal{L}_1(z_m) + \mathcal{N}_1(z_0 + z_1 + \cdots + z_m) - \mathcal{N}_1(z_0 + z_1 + \cdots + z_{m-1})\big\}. \end{aligned}$$

Thus, we have

$$\sum_{k=0}^{\infty}\mathcal{L}_1[z_{k+1} - z_k] = -\mathcal{L}\left[\sum_{k=0}^{\infty} z_k\right] - \mathcal{N}\left[\sum_{k=0}^{\infty} z_k\right] - z_0. \tag{21}$$

We can see from (19) and (21) that $y(p,t) = \sum_{k=0}^{\infty} z_k$ is the solution of (6).

Let $\sum_{k=0}^{m} z_k$ is the approximated solution of (6). From (17), we have

$$\|\mathcal{A}_k - \mathcal{A}_m\| \leq \frac{1-\varphi^{k-m}}{1-\varphi}\varphi^{m+1}\|z_0\|.$$

As $k \to \infty$ then $\mathcal{A}_k \to y(p,t)$. Thus, we get

$$\mathcal{E}_k = \|y(p,t) - \sum_{k=0}^{m} z_k\| \leq \frac{1}{1-\varphi}\varphi^{m+1}\|z_0\|.$$

Since $0 < \varphi < 1$, thus $1 - \varphi^{k-m} < 1$. This completes the proof. □

4. Numerical results

In this section, we test the accuracy of the proposed approach (MVIM) for an aggregation equation by applying it to various physically relevant and analytically tractable kernels. The series solution obtained by MVIM is compared with the recent work of Arora et al. [38] on VIM and exact solutions for analytically tractable kernels. Due to the non-availability of the exact solutions for the physically relevant kernels, the testing of MVIM is done against the finite volume scheme [48]. We also calculate the integral moments of the number density function which is important to access the important properties of the system. Mathematically, they can be calculated by the following relation:

$$\mu_j = \int_0^\infty p^j \; y(p,t) \; dp \qquad j = 0, 1, \dots . \tag{22}$$

The zeroth (μ_0) and first (μ_1) order moments represent the total number and total mass of the particles in the system, respectively.

Additionally, to verify the accuracy of iterative methods, the truncation error (σ) between the exact solution $y(p,t)$ and approximate solution $y_k(p,t)$ is evaluated by using the following relation [34]:

$$\sigma = \sum_{j=1}^{1000} |y_k^j - y_j| h_j, \tag{23}$$

where $y_k^j = y_k(p_j,t)$, $y_j = y(p_j,t)$. First, we divide the interval $]0,\infty[$ into 1000 (chose randomly) intervals $[p_{j-\frac{1}{2}}, p_{j+\frac{1}{2}}]$ for $j = 0, 1, \dots, 1000$. Now, $h_j = p_{j-\frac{1}{2}} - p_{j+\frac{1}{2}}$ and $p_j = \frac{p_{j-\frac{1}{2}} + p_{j+\frac{1}{2}}}{2}$ is the midpoint of the interval. All simulations are performed on an Intel Core i7-1255U CPU at 1.70 GHz with 16.00 GB of RAM using MATLAB R2019a software.

Example 4.1. Consider the constant kernel $l(p,q) = 1$ for Eqs. (1)–(2) with an exponential initial distribution $y_0(p) = e^{-p}$.

The constant kernel has been used to simulate protein aggregation and other biomolecule aggregation during biopharmaceutical manufacturing and formulation [49]. For the constant kernel, the iterative formula for MVIM (12) reduces to

$$y_{k+1}(p,t) = y_k(p,t) - \int_0^t e^{\eta - t}\left[\frac{\partial y_k(p,\eta)}{\partial \eta} - \frac{1}{2}\int_0^p y_k(p-q,\eta) y_k(q,\eta) dq + \int_0^\infty y_k(p,\eta) y_k(q,\eta) dq\right] d\eta. \tag{24}$$

As a result, the first few iterations are determined as

$$y_1(p,t) = \mathrm{e}^{-p}\left(1 + \frac{(p-2)\,(1-\mathrm{e}^{-t})}{2}\right),$$

$$y_2(p,t) = \mathrm{e}^{-p}\left(\frac{p}{4} + \frac{p^3}{48} + \mathrm{e}^{-t}\left(\frac{t}{2} + \frac{(p-2)}{2} - \frac{p^2}{4} + \frac{p^2 t}{4} - \frac{p^3 t}{24} - \frac{pt}{2}\right) + \mathrm{e}^{-2t}\left(\frac{1}{2} - \frac{3p}{4} + \frac{p^2}{4} - \frac{p^3}{48}\right)\right),$$

$$\begin{aligned} y_3(p,t) = \mathrm{e}^{-p}\Bigg(1 &- \frac{11p}{32} + \frac{(p-2)}{2} + \frac{7p^3}{384} + \frac{p^5}{3840} + \frac{p^7}{645120} + \mathrm{e}^{-t}\Bigg(-\frac{55}{192} + \frac{7p}{96} - \frac{3t}{16} + \frac{11p^2}{384} + \frac{95p^3}{1152} - \frac{97p^4}{4608} + \frac{13p^5}{11520} + \frac{19p^6}{138240} + \frac{19p^7}{1935360} + \frac{5t^2}{32} \\ &- \frac{1}{2} - \frac{3pt^2}{16} - \frac{11p^2 t}{32} + \frac{5p^3 t}{96} - \frac{p^4 t}{384} + \frac{p^5 t}{1920} - \frac{p^6 t}{11520} + p + \frac{t}{2} + \frac{7p^2 t^2}{64} - \frac{5p^3 t^2}{192} + \frac{p^4 t^2}{256} - \frac{p^5 t^2}{1920} + \frac{p^6 t^2}{23040} - \frac{p^7 t^2}{322560} - \frac{(p-2)}{2} - \frac{p^2}{4} + \frac{11pt}{16} \\ &+ \frac{p^2 t}{4} - \frac{p^3 t}{24} - \frac{pt}{2}\Bigg) + \mathrm{e}^{-2t}\Bigg(\frac{1}{16} + \frac{p}{2} + \frac{5t}{8} - \frac{9p^2}{32} - \frac{7p^3}{192} + \frac{7p^4}{384} - \frac{p^5}{960} + \frac{p^6}{11520} - \frac{p^7}{107520} + \frac{t^2}{8} + \frac{1}{2} - \frac{pt^2}{4} + \frac{7p^2 t}{16} - \frac{p^3 t}{8} + \frac{p^4 t}{64} - \frac{p^5 t}{960} \\ &+ \frac{p^6 t}{5760} - \frac{p^7 t}{80640} - \frac{3p}{4} + \frac{3p^2 t^2}{16} - \frac{7p^3 t^2}{96} + \frac{p^4 t^2}{64} - \frac{p^5 t^2}{480} + \frac{p^6 t^2}{5760} + \frac{p^2}{4} - \frac{p^7 t^2}{161280} - \frac{p^3}{48} - \frac{7pt}{8}\Bigg) + \mathrm{e}^{-3t}\Bigg(\frac{13}{64} - \frac{13p}{32} + \frac{3t}{32} + \frac{23p^2}{128} - \frac{5p^3}{384} - \frac{5p^4}{1536} \\ &+ \frac{p^5}{3840} + \frac{p^6}{46080} - \frac{p^7}{645120} + \frac{13p^2 t}{64} - \frac{5p^3 t}{64} + \frac{13p^4 t}{768} - \frac{p^5 t}{480} + \frac{p^6 t}{7680} - \frac{p^7 t}{322560} - \frac{pt}{4}\Bigg) + \mathrm{e}^{-4t}\Bigg(\frac{1}{48} - \frac{7p}{96} + \frac{7p^2}{96} - \frac{35p^3}{1152} + \frac{7p^4}{1152} - \frac{7p^5}{11520} \\ &+ \frac{p^6}{34560} - \frac{p^7}{1935360}\Bigg)\Bigg), \end{aligned}$$

and so on. The exact solution of (1) with constant kernel [50] is given by

$$y(p,t) = \frac{4\exp\left(-\frac{2p}{2+t}\right)}{(2+t)^2}. \tag{25}$$

Fig. 1 shows a comparison of the fifth iterative term derived using HAM [36], VIM [38] and MVIM with the exact solutions (25). It can be observed that for a short time domain (ends with $t = 0.85$), VIM, HAM and MVIM coincide with the exact solution, but for a longer time domain (ends with $t = 4$), the MVIM is more accurate than both VIM and HAM (see Fig. 1(a)). It is worth mentioning that the existing VIM and HAM captures the solution accurately by consuming five series terms till time $t = 1$ [13,38] whereas the MVIM captures the result with higher precision till time $t = 4$ using the same series terms. Among VIM and HAM, HAM performs better than the VIM for the longer time domain. Moreover, the new approach capture the zeroth and first order moments more accurately than the VIM as demonstrated in Fig. 1(b). For different values of k, the truncation error (23) is determined for $t = 4$ and $p \in [0, 10]$ in Table 1. One can observe that the error decreases as the number of series terms (k) increases, and the MVIM provided lesser truncation error than both VIM and HAM.

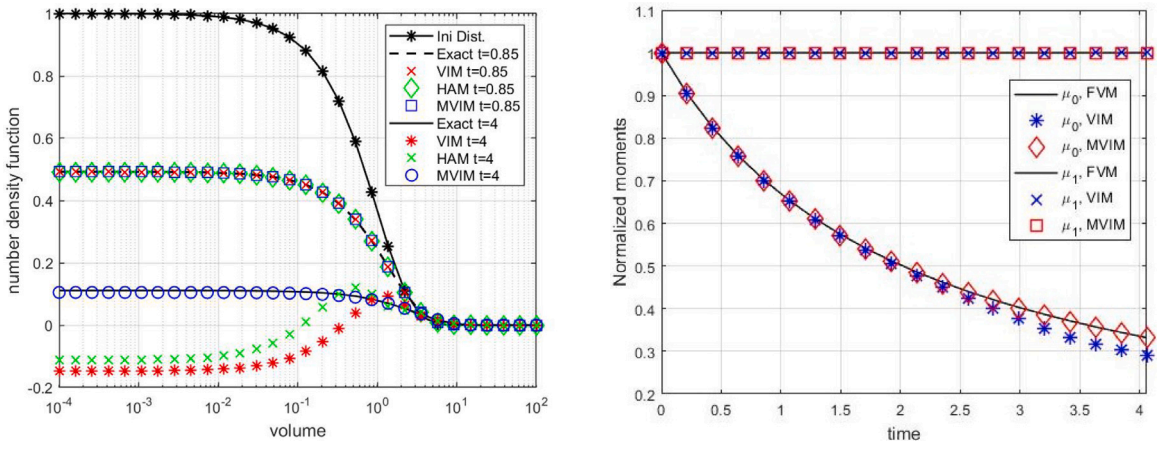

(a) Number density function (b) Normalized Moments

Fig. 1. Comparison between VIM, HAM, MVIM and exact solutions for constant kernel with $y_0 = e^{-p}$ at time $t = 0.85$ and $t = 4$.

Table 1
Truncation error for constant kernel at $t = 4$ and $p \in [0, 10]$.

k	$k = 2$	$k = 3$	$k = 4$	$k = 5$
VIM	0.94732	0.59636	0.25925	0.11228
HAM	0.38310	0.22265	0.12380	0.06546
MVIM	0.12841	0.061132	0.028116	0.012273

Table 2
Truncation error for sum kernel at $t = 2$ and $p \in [0, 10]$.

k	$k = 2$	$k = 3$	$k = 4$
VIM	2.92243	2.90527	2.76710
OVIM	0.222678	0.181348	0.130519
MVIM	0.20460	0.051121	0.019209

Example 4.2. Consider the sum kernel $l(p, q) = p + q$ for the Eqs. (1)–(2) with exponential initial distribution $y_0(p) = e^{-p}$.

The sum kernel is used to model the aggregation and coagulation of atmospheric particles such as dust soot, and aerosols [51]. The exact solution of aggregation Eq. (1) for a sum kernel [52] is given by

$$y(p,t) = \frac{(1-\sigma(t))e^{-(1+\sigma(t))p}}{p\sqrt{\sigma(t)}} \mathcal{I}_1(2p\sqrt{\sigma(t)}), \tag{26}$$

where, $\mathcal{I}(t)$ is the modified Bessel function of the first kind and $\sigma(t) = 1 - e^{-t}$. For the sum kernel, the iterative formula for MVIM (12) reduces to

$$y_{k+1}(p,t) = y_k(p,t) - \int_0^t e^{\eta - t}\left[\frac{\partial y_k(p,\eta)}{\partial \eta} - \frac{1}{2}\int_0^p p y_k(p-q,\eta) y_k(q,\eta) dq + \int_0^\infty (p+q) y_k(p,\eta) y_k(q,\eta) dq\right] d\eta. \tag{27}$$

By using the above relation, we get the following iterations

$$y_1(p,t) = \mathrm{e}^{-p}\left(1 - \frac{\mathrm{e}^{-t}\left(\mathrm{e}^t - 1\right)\left(-p^2 + 2p + 2\right)}{2}\right),$$

$$y_2(p,t) = \mathrm{e}^{-p}\left(1 + p - \frac{p^2}{2} + \frac{p^4}{12} - \frac{p^5}{24} + \frac{p^6}{240} + \mathrm{e}^{-t}\left(-2p + tp^2 - tp^3 + \frac{tp^5}{12} - \frac{tp^6}{120} + p^3 - \frac{p^4}{6}\right) + \mathrm{e}^{-2t}\left(p + \frac{p^2}{2} - p^3 + \frac{p^4}{12} + \frac{p^5}{24} - \frac{p^6}{240}\right)\right.$$
$$\left. - \frac{(1-\mathrm{e}^{-t})(-p^2 + 2p + 2)}{2}\right),$$

and so on. In Fig. 2, the exact solution (26) and the numerical solution obtained by VIM, OVIM [38] and MVIM using four series terms for the sum kernel have been plotted. MVIM provides excellent agreement with the exact solution while OVIM and VIM show deviation from the exact solution (refer to Fig. 2(a)) and possibly requires more series terms to find an accurate solution that leads to high computational cost. In addition, the normalized moments estimated by the MVIM show higher accuracy than the VIM as demonstrated in Fig. 2(b). In Table 2, the truncation errors between the exact and numerical solutions are summarized for different order of series terms k with a range of $p \in [0, 10]$ at $t = 2$ for the sum kernel. Once again, MVIM proved to be a better approach in estimating errors for different series term solutions than both VIM and HAM.

Example 4.3. Consider the polymerization kernel $l(p, q) = (p^{\frac{1}{3}} + c)(q^{\frac{1}{3}} + c)$ with $c = 0$ for the Eqs. (1)–(2) with an exponential initial distribution $y_0(p) = e^{-p}$ and gamma initial distribution $y_0(p) = 4pe^{-2p}$.

The polymerization kernel has been used in solving problems arise related to emulsion polymerization and particle formation in combustion processes [53]. The analytical (exact) solution for the polymerization kernel is not available in the literature, thus the result are compared with

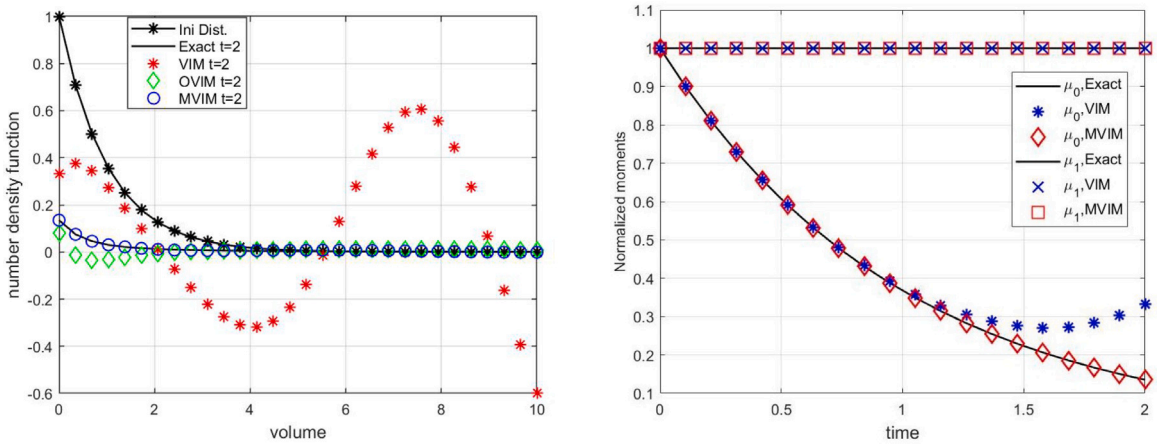

(a) Number density function (b) Normalized Moments

Fig. 2. Comparison between VIM, OVIM, MVIM and exact solution for sum kernel with $y_0 = e^{-p}$ at time $t = 2$.

the finite volume scheme [48] to test the accuracy of the MVIM. For the polymerization kernel, the iterative formula for MVIM (12) reduces to

$$y_{k+1}(p,t) = y_k(p,t) - \int_0^t e^{\eta - t}\left[\frac{\partial y_k(p,\eta)}{\partial \eta} - \frac{1}{2}\int_0^p (p-q)^{\frac{1}{3}} q^{\frac{1}{3}} y_k(p-q,\eta) y_k(q,\eta) dq + p^{\frac{1}{3}} \int_0^\infty q^{\frac{1}{3}} y_k(p,\eta) y_k(q,\eta) dq\right] d\eta. \tag{28}$$

By using the above relation and exponential initial distribution $y_0(p) = e^{-p}$, we get the following iterations

$$y_1(p,t) = e^{-p}\left(1 - \frac{2^{1/3} e^{-p}(e^t - 1)\sqrt{\pi} p^{1/3}\left(\sqrt{3}\pi p^{-4/3} - 10\Gamma(-2/3)^2\right)}{5\Gamma(-1/6)\Gamma(2/3)}\right),$$

$$\begin{aligned} y_2(p,t) = e^{-p}\Bigg(1 &- \frac{4\pi p^{1/3}(1-e^{-t})}{9\sqrt{3}} + \frac{\pi^2 p^2 (1-e^{-t})}{9\Gamma(-4/3)} + \frac{81\pi^3 p^2 (e^{-2t}-1)\left(120 - p\iota\tau^3\right)}{2^{1/3} 4000 \Gamma(-4/3)^2 \Gamma(-1/6)^2} + \frac{\pi^{3/2}(e^{-t}-1)}{5\Gamma(-1/6)\Gamma(-4/3)} + \frac{27\pi^{5/2} p^{2/3}}{\Gamma(-1/6)\Gamma(-4/3)^2} \\ &\left(\frac{(2e^{-2t} - 2 - p^{4/3}(e^{-t}-1))}{2^{5/3}10} - \frac{27p^3(e^{-2t}-1)}{2^{2/3}8000}\right) + \frac{2^{7/3}\pi^{3/2} p^{2/3}(e^{-t}-1)}{3\sqrt{3}\Gamma(-1/6)}\left(2^{1/3}\pi p^2 + \frac{243\sqrt{3}p^{10/3}}{280} - \frac{9\sqrt{3}p^{1/3}(1+p^{4/3})}{2^{2/3}} + \frac{2^{1/3}\sqrt{3}\pi^{3/2}p^{5/3}}{5\Gamma(-1/6)\Gamma(2/3)}\right) \\ &+ \frac{27\sqrt{3}(e^{-2t}-1)\Gamma(7/6)^2 p^{11/3}}{2^{1/3}(2200)} - \frac{2^{7/3}\sqrt{\pi} p^{1/3}\Gamma(2/3)(e^{-t}-1)}{\Gamma(-1/6)} - \frac{\pi p^{7/3}\Gamma(5/3)(e^{-2t}-1)}{14\sqrt{3}} + \Gamma(7/3)p^{1/3}\left(\frac{3(e^{-t}-1)}{4} + \frac{\pi p^{1/3}(e^{2t}-1)}{3\sqrt{3}}\right) \\ &+ te^{-t}\left(\frac{-4\pi p^{1/3}}{9\sqrt{3}} + \frac{\pi^2 p^2}{9\Gamma(-4/3)} + \frac{2^{7/3}\pi^{3/2}p^{2/3}}{3\sqrt{3}\Gamma(-1/6)} + \frac{27\pi^{5/2}p^{2/3}}{2^{2/3}5\Gamma(-1/6)\Gamma(-4/3)^2}\left(1 - \frac{p^{4/3}}{4} - \frac{27p^3}{880}\right) + \frac{\pi^{3/2}p^{1/3}}{2^{2/3}5\Gamma(-1/6)\Gamma(-4/3)}\left(9\sqrt{3}\left(\frac{p^{4/3}}{2} - 1\right)\right.\right. \\ &\left.\left. + 4\pi p^{5/3} + \frac{243\sqrt{3}p^3}{280}\right) + \frac{\pi\Gamma(5/3)p^{7/3}}{7\sqrt{3}} + \frac{3p^{1/3}\Gamma(7/3)}{4} + \frac{27\sqrt{3}\Gamma(7/6)^2 p^{11/3}}{2^{1/3}1100} + \frac{2\pi p^{2/3}}{3\sqrt{3}} + \frac{\pi^3 p^2 \Gamma(-1/6)^2}{2^{1/3}50\Gamma(-4/3)^2}\left(243 - \frac{81p^3}{40}\right)\right)\Bigg). \end{aligned}$$

The results obtained by VIM and MVIM using two series terms of the truncated series at different times are compared with the finite volume scheme (FVS) in Fig. 3. It can be seen that both VIM and MVIM coincide with the solution of FVS for a short time $t = 0.31$, however, for a longer time $t = 1.5$, MVIM outperforms VIM and the result overlaps with the exact solution (see Fig. 3(a)). It is worth mentioning that the MVIM took only 86s CPU time for obtaining the solutions. The accuracy of the VIM can be improved to the desired level by considering more series terms in the truncated series, but at a high computational cost. In addition, the zeroth and first order moments which play significant role in computing the total number and total volume in the system are very well captured by MVIM compared to traditional VIM.

Now, the new series solutions of the polymerization kernel with gamma initial distribution $y_0(p) = 4pe^{-2p}$ are obtained. Following the same procedure, we get the following iterations

$$y_1(p,t) = 4e^{-2p}p\left(1 - \frac{8(1-e^{-p})\sqrt{\pi}p^{1/3}(2^{1/3}9\sqrt{3}\pi p^{7/3} + 55\Gamma(-1/3)\Gamma(2/3))}{495\,\Gamma(-1/6)\Gamma(2/3)}\right),$$

$$\begin{aligned} y_2(p,t) = 8e^{-2p}p\Bigg(&\frac{1}{2} + 2^{1/3}(1-e^{-t})\sqrt{\pi}p^{1/3}\left(\frac{2^{2/3}5\sqrt{\pi}}{81\sqrt{3}} + \frac{80\pi^{3/2}2^{1/3}p^{8/3}}{2187\Gamma(-1/3)} + \frac{8748\sqrt{3}\pi p^5}{475475\Gamma(-1/3)\Gamma(-1/6)} - \frac{2^{4/3}\Gamma(1/3)}{9\sqrt{\pi}} - \frac{36\sqrt{3}\pi}{55\Gamma(-1/3)\Gamma(-1/6)}\right. \\ &\left. - \frac{6p^{7/3}\Gamma(1/3)}{55\Gamma(-1/6)} - \frac{4\pi p^{7/3}}{55\Gamma(-1/6)\Gamma(2/3)} + \frac{16\sqrt{\pi}p^{8/3}\Gamma(1/3)}{55\sqrt{3}\Gamma(-1/6)} - \frac{2^{5/3}\Gamma(-1/3)}{9\Gamma(-1/6)} + \frac{2p^{1/3}\Gamma(1/3)^2}{81\sqrt{\pi}}\right) + p^{2/3}\pi^2(1-e^{-2p})\left(-\frac{3888\sqrt{3}2^{1/3}p^5}{359975}\right. \\ &- \frac{2592\pi 2^{2/3}p^{7/3}}{3025\Gamma(1-/3)^2\Gamma(-1/6)^2} + \frac{32\sqrt{32}^{1/3}}{55} + \frac{32\sqrt{\pi}2^{1/3}p^{7/3}}{297\Gamma(1-/3)\Gamma(-1/6)} + \frac{2^{1/3}80p^{8/3}}{7371\Gamma(1/3)} - \frac{2^{2/3}40\Gamma(1/3)}{729\sqrt{3\pi}}\Bigg) + e^{-t}\left(-\frac{2^{2/3}80\pi p^4}{2187\Gamma(-1/3)} - \frac{20p^{4/3}}{81\sqrt{3}}\right. \\ &\left.\left. + \frac{3^{1/3}32\sqrt{3}\pi p^{5/3}}{55\Gamma(-1/6)^2}\left(2 - \frac{245p^5}{6545}\right)\right) - \frac{2^{2/3}192\pi^2 p^4\left(p^5 - 945\right)}{3025 * 35\Gamma(-1/3)^2\Gamma(-1/6)^2} + \frac{2^{1/3}p}{\sqrt{\pi}\Gamma(-1/3)\Gamma(-1/6)}\left(\frac{64\pi p^3}{297} - \frac{12\sqrt{3}p^{1/3}}{55}\left(p^{7/3} - 3 + \frac{729p^5}{8645}\right)\right)\Bigg) \end{aligned}$$

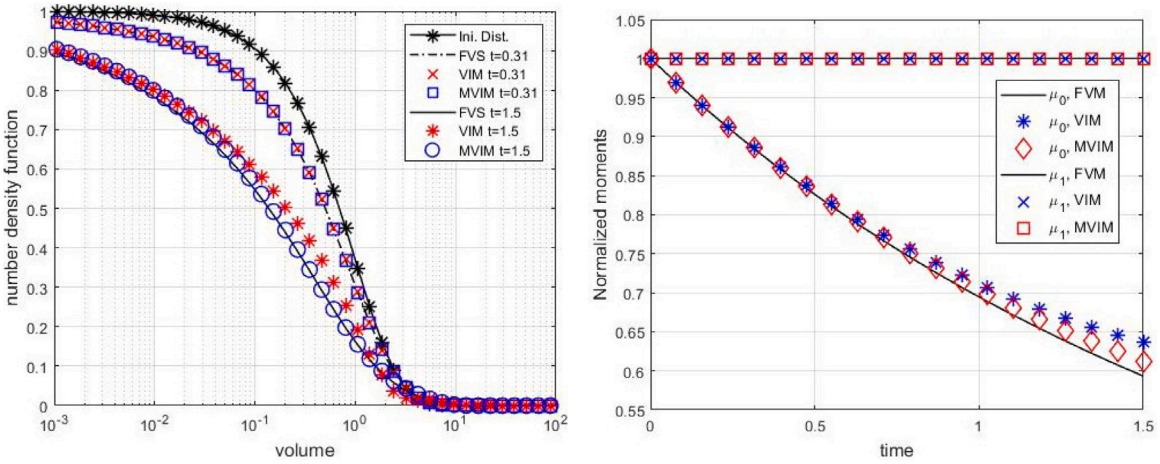

(a) Number density function (b) Moments

Fig. 3. Testing of VIM, MVIM and FVS solution for Polymerization kernel with $y_0 = e^{-p}$ at time $t = 0.31$ and $t = 1.5$.

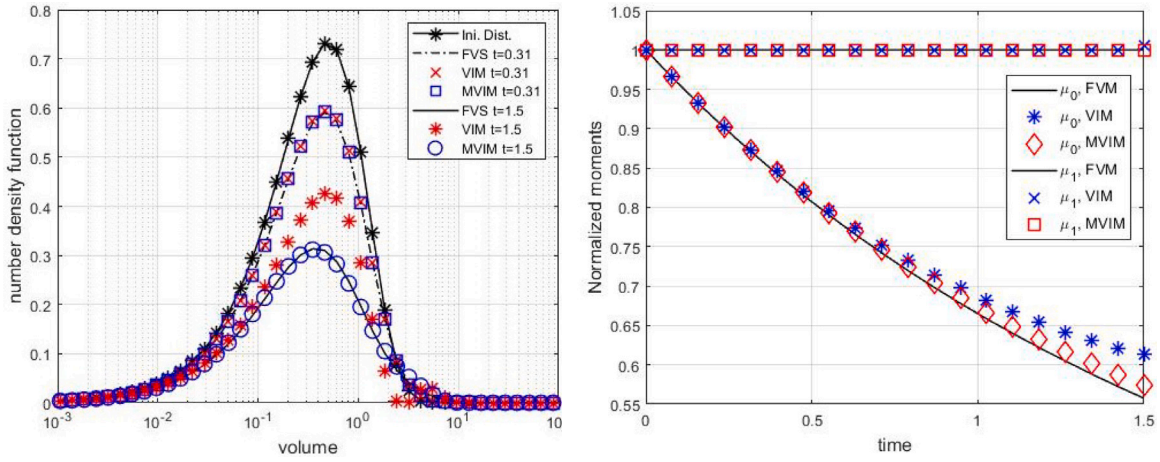

(a) Number density function (b) Moments

Fig. 4. Testing of VIM, MVIM and FVS solution for Polymerization kernel with $y_0 = 4pe^{-2p}$ at time $t = 0.31$ and $t = 1.5$.

$$-\frac{2^{1/3}160p^{13/3}}{7371\Gamma(1/3)}+\frac{2^{2/3}\Gamma(1/3)p^{4/3}}{9\pi^2}\left(1+\frac{80\pi p^{1/3}}{81\sqrt{3}}\right)-\frac{2^{7/3}p^2}{\pi^2}\left(\frac{p^{2/3}\Gamma(1/3)^2}{81}+\frac{4\pi p^2\Gamma(7/6)}{55\sqrt{3}\Gamma(-1/6)}\right)\Bigg).$$

Similar to the previous case, the VIM and MVIM solutions obtained using two terms of the truncated series are compared against the FVS solution at $t = 0.31$ and $t = 1.5$ for the polymerization kernel with $y_0 = 4pe^{-2p}$ in Fig. 4. MVIM solution took only $48s$ CPU time for finding the solution and shows excellent agreement with the FVS solution over VIM for both shorter and longer times as depicted in Fig. 4(a). Furthermore, MVIM computed the zeroth and first order moment (plotted in Fig. 4(b)) more accurately than VIM. This illustrates that the MVIM has the tendency to capture the longer time solutions as well as moments by consuming few terms of the truncated series.

Example 4.4. Consider the Pulvermacher aggregation kernel $l(p,q) = p^{\frac{2}{3}} + q^{\frac{2}{3}}$ for the Eqs. (1)–(2) with ICs $y_0(p) = e^{-p}$ and $y_0(p) = 4pe^{-2p}$.

This kernel has been used in modelling different processes that occur in materials science, chemical engineering and aerosol science [54]. The exam solution for polymerization kernel does not exist in the literature.

For the Pulvermacher kernel, the iterative formula for MVIM (12) reduces to

$$y_{k+1}(p,t) = y_k(p,t) - \int_0^t e^{\eta - t}\left[\frac{\partial y_k(p,\eta)}{\partial \eta} - \frac{1}{2}\int_0^p ((p-q)^{\frac{2}{3}} + q^{\frac{2}{3}})y_k(p-q,\eta)y_k(q,\eta)dq + \int_0^\infty (p^{\frac{2}{3}} + q^{\frac{2}{3}})y_k(p,\eta)y_k(q,\eta)dq\right]d\eta. \tag{29}$$

By using the above relation with exponential initial distribution $y_0(p) = e^{-p}$, we get the following iterations

$$y_1(p,t) = e^{-p}\left(1 + \frac{(1-e^{-t}(p^{2/3}(3p-5) - 5\Gamma(5/3)))}{5}\right),$$

$$y_2(p,t) = e^{-p}\left(1 + (e^{-t}-1)\left(2p^{2/3} - p^{4/3} - \frac{6p^{5/3}}{5} + \frac{36p^{7/3}}{35} - \frac{9p^{10/3}}{50}\right) - \frac{(e^{-2t}-1)\pi p^3}{\sqrt{3}}\left(\frac{8}{81} - \frac{8p}{135} + \frac{14p^2}{2025} + \frac{\sqrt{3}p^{1/3}\Gamma(-1/3)}{50\pi}\right)\right.$$

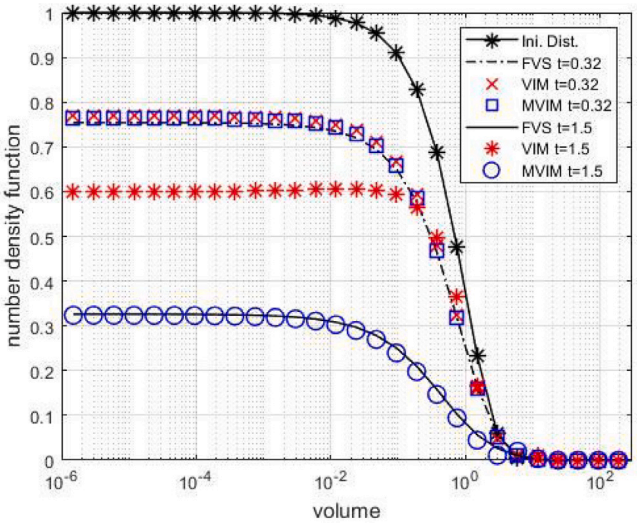

Fig. 5. Comparison between VIM, MVIM and FVS solution for Pulvermacher kernel with $y_0 = e^{-p}$ at time $t = 0.32$ and $t = 1.5$.

$$+\frac{2^{2/3}\Gamma(5/6)p^{7/3}\sqrt{3\pi}(10-3p)((e^{-t}-1)+\Gamma(5/3)(e^{-2t}-1))}{70\Gamma(1/3)}+(e^{-t}-1)\Gamma(5/3)\left(2-3p^{2/3}+\frac{9p^{5/3}}{5}-2\Gamma(5/3)+\frac{2\Gamma(7/3)}{5\Gamma(5/3)}\right)+(e^{-2t}-1)$$
$$\Gamma(5/3)p^{2/3}\left(p^{2/3}\left(1-\frac{36p}{35}+\frac{9p^2}{100}\right)+2\Gamma(5/3)\left(1-\frac{6p}{5}+\Gamma(5/3)\right)-\frac{2\Gamma(7/3)}{5\Gamma(5/3)}\left(1-\frac{3p}{5}+\Gamma(5/3)\right)\right)+te^{-t}\left(p^{2/3}\left(1-p^{2/3}-\frac{3p}{5}\right.\right.$$
$$+\frac{36p^{5/3}}{35}-\frac{9p^{8/3}}{50}\Big)-\frac{\pi p^3}{\sqrt{3}}\left(\frac{16}{81}-\frac{16p}{135}+\frac{28p^2}{2025}\right)+\frac{2^{2/3}\sqrt{3\pi}p^{7/3}\Gamma(5/6)}{7\Gamma(1/3)}\left(1-\frac{6p}{5}+\frac{\Gamma(5/3)(10-3p)}{5}\right)+\Gamma(5/3)\left(1-3p^{2/3}+2p^{4/3}\right.$$
$$\left.\left.+\frac{9p^{5/3}}{5}-\frac{72p^{7/3}}{35}+\frac{9p^{10/3}}{25}\right)-2\Gamma(5/3)^2\left(1-2p^{2/3}+\frac{6p^{5/3}}{5}-\Gamma(5/3)+\frac{4\Gamma(7/3)}{5}\right)+\Gamma(7/3)\left(\frac{2}{5}-\frac{4p^{2/3}}{5}+\frac{12p^{5/3}}{25}\right)\right)\Big).$$

The comparison of the second iterative term of VIM and MVIM with the FVS solution for the Pulvermacher kernel is shown in Fig. 5. One can see that both VIM and MVIM agree with the FVS solution for short periods of time $t = 0.32$, however for longer time as $t = 1.5$, MVIM leads to a powerful technique that predicts results with high accuracy than VIM. Moreover, only $52s$ CPU time required to obtained the MVIM solution for the complex Pulvermacher aggregation kernel.

Now, we consider the Pulvermacher kernel for the Eqs. (1)–(2) with initial gamma distribution $y_0(p) = 4e^{-2p}p$. By using (29), we get the following iterations

$$y_1(p,t) = e^{-2p}\left(4p+\frac{(2p)^{4/3}(1-e^{-t})(-22p^{1/3}+9p^{7/3}-11\Gamma(8/3))}{11}\right),$$
$$y_2(p,t) = e^{-2p}p\left(4+(1-e^{-t})\left(4p^{7/3}-8p^{5/3}+\frac{36p^{11/3}}{11}-\frac{1962p^{13/3}}{715}+\frac{81p^{19/3}}{418}-\frac{3p\Gamma(11/3)(1-3p^{2/3})}{2^{5/3}}-\frac{2^{2/3}10\sqrt{3}\pi p^{13/3}\Gamma(5/6)(76-9p^2)}{1729\Gamma(1/3)}\right.\right.$$
$$-2^{4/3}p\Gamma(8/3)(1-2^{1/3}\Gamma(8/3))-\frac{27p^{11/3}\Gamma(11/3)}{2^{2/3}44}-\frac{63p\Gamma(13/3)}{2^{2/3}220}\Big)+(1-e^{-2t})\left(\frac{980\pi p}{891\sqrt{3}}+\frac{16\pi p^5}{729\sqrt{3}}\left(14-\frac{109p^2}{33}+\frac{65p^4}{594}\right)\right.$$
$$-\frac{2^{2/3}72\sqrt{3}p^{19/3}\Gamma(11/6)^2}{1729}+2^{2/3}p^{5/3}\Gamma(8/3)^2\left(-2+\frac{9p^2}{11}+\frac{2^{1/3}27p^{8/3}}{91\sqrt{\pi}\Gamma(5/6)^{-1}}\right)-p\Gamma(8/3)^3-\frac{3p^{7/3}\Gamma(11/3)(22-9p^2)}{2^{2/3}44}+$$
$$\left.\frac{63p^{5/3}\Gamma(13/3)(22-9p^2)}{2^{1/3}4840}\right)+te^{-t}\left(-\frac{1960\pi p}{891\sqrt{3}}+4p^{5/3}(1-p^{2/3})-\frac{18p^{11/3}\left(65-109p^{2/3}\right)}{715}-\frac{4\pi p^5}{729\sqrt{3}}\left(111-\frac{872p^2}{33}+\frac{280p^4}{297}\right)-\right.$$
$$\frac{81p^{19/3}}{418}+\frac{2^{1/3}\pi p^{11/3}}{\sqrt{3}\Gamma(1/3)}\left(\frac{40}{11}-\frac{32p^{2/3}}{13}\right)+\frac{30\sqrt{3}\pi p^{19/3}}{209\Gamma(1/3)}+\frac{2^{2/3}10\sqrt{3}\pi p^{13/3}\Gamma(5/6)(190-9p^2)}{1729\Gamma(1/3)}+\frac{2^{2/3}144\sqrt{3}p^{19/3}\Gamma(11/6)^2}{1729}-2^{5/3}p\Gamma(8/3)^2$$
$$\left.\left.\left(1-2p^{2/3}+\frac{9p^{8/3}}{11}+\frac{54p^{10/3}\Gamma(5/6)}{2^{2/3}91\sqrt{\pi}}-\frac{\Gamma(8/3)}{2^{2/3}}\right)+\frac{3p}{2^{5/3}}\Gamma(11/3)\left(1-3p^{2/3}+2p^{4/3}+\frac{9p^{8/3}}{22}-\frac{9p^{10/3}}{11}\right)+\frac{63p\Gamma 13/3}{2^{1/3}220}\left(\frac{1}{2}-p^{2/3}+\frac{9p^{8/3}}{22}\right)\right)\right).$$

Fig. 6 shows the comparison of FVS against the VIM and MVIM for the Pulvermacher kernel. One again, for short time intervals of $t = 0.32$, the results estimated by both VIM and MVIM match well with FVS. However for longer time $t = 1.5$, MVIM yields more accurate results than VIM by consuming $240s$ CPU time. This results show that not the analytically tractable kernels (sum and product kernels), this approach has the tendency to capture the series solution accurately by consuming fewer series terms for the physically relevant kernels. This demonstrates that the MVIM is very effective in handling complex structured kernels that have been used to model real-life applications including granulation and crystallization processes within chemical and pharmaceutical sciences.

Example 4.5. Consider the product kernel for the Eqs. (1)–(2), that is, $l(p,q) = pq$ with exponential initial distribution $y_0(p) = e^{-p}$ and $y_0(p) = e^{-p}/p$.

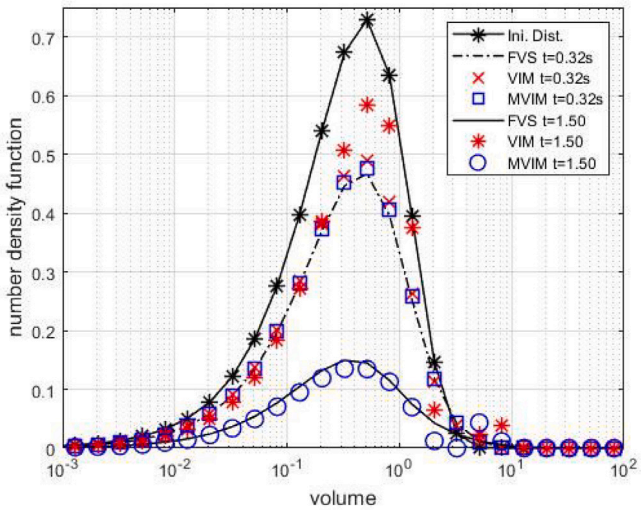

Fig. 6. Comparison between VIM, MVIM and FVS solution for Pulvermacher kernel on semilog scale with $y_0 = 4pe^{-2p}$ at time $t = 0.32$ and $t = 1.5$.

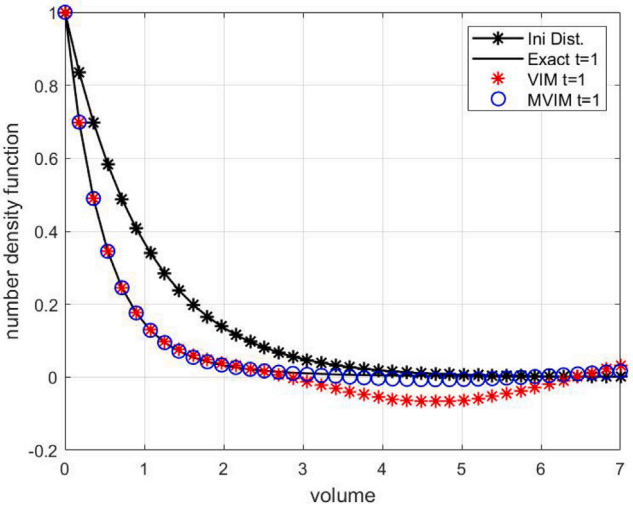

Fig. 7. Comparison between VIM, MVIM and analytic solution for product kernel with $y_0 = e^{-p}$ at time $t = 1$.

The product kernel has been used in the past for tracking the dynamics of the casein micelles during enzymic coagulation while cheese manufacturing in the dairy processes [55]. For the product kernel, the iterative formula for MVIM (12) reduces to

$$y_{k+1}(p,t) = y_k(p,t) - \int_0^t e^{\eta - t}\left[\frac{\partial y_k(p,\eta)}{\partial \eta} - \frac{1}{2}\int_0^p (p-q)q y_k(p-q,\eta)y_k(q,\eta)dq + p\int_0^\infty q y_k(p,\eta)y_k(q,\eta)dq\right]d\eta. \tag{30}$$

For the product kernel with initial iteration $y_0(p) = e^{-p}$, from (30) we get the following iterations

$$y_1(p,t) = \mathrm{e}^{-p}\left(1 + p(\mathrm{e}^{-t} - 1) - \frac{p^3(\mathrm{e}^{-t} - 1)}{12}\right),$$

$$y_2(p,t) = \mathrm{e}^{-2p}\left(1 - 2p + p^2 + \frac{p^3}{6} - \frac{p^4}{6} + \frac{p^5}{60} + \frac{p^6}{360} - \frac{p^7}{1260} + \frac{p^9}{181440} + \mathrm{e}^{-t}\left(p - p^2(1+t) - \frac{p^3}{12} + \frac{p^4}{6} - \frac{p^6}{360} - \frac{p^3 t}{12} + \frac{p^4 t}{6} - \frac{p^5 t}{30} - \frac{p^6 t}{360} + \frac{p^7 t}{630} - \frac{p^9 t}{90720} + pt + p - \frac{p^3}{12}\right) + \mathrm{e}^{-2t}\left(\frac{p^7}{1260} - \frac{p^5}{60} - \frac{p^9}{181440}\right)\right),$$

and so on. The exact solution for product kernel with $y_0(p) = e^{-p}$ is as follow [56]:

$$y(p,t) = e^{-(t+1)p}\sum_{k=0}^{\infty}\frac{t^k p^{3k}}{(k+1)!\Gamma(2k+2)}. \tag{31}$$

The computed β_i's for the product kernel are as follows [45,57]:

$$\beta_1 = \frac{\|z_1\|}{\|z_0\|} = \frac{\|y_2 - y_1\|}{\|y_1 - y_0\|} = 0.46230$$

Table 3
Truncation error for product kernel at $t = 1$ and $p \in [0, 7]$.

k	$k = 2$	$k = 3$	$k = 4$
VIM	0.329794	0.269501	0.185893
MVIM	0.092679	0.049648	0.0292537

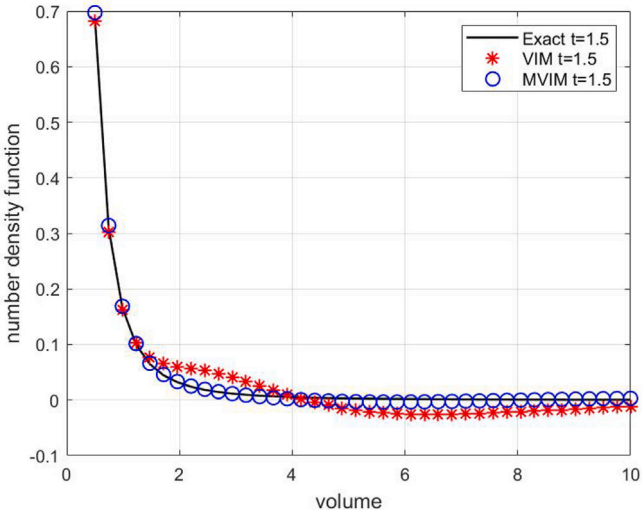

Fig. 8. Comparison between VIM, MVIM and exact solution for product kernel with $y_0 = e^{-p}/p$ at time t = 1.5.

$$\beta_2 = \frac{\|z_1\|}{\|z_0\|} = \frac{\|y_3 - y_2\|}{\|y_2 - y_1\|} = 0.22470$$
$$\beta_3 = \frac{\|z_3\|}{\|z_2\|} = \frac{\|y_4 - y_3\|}{\|y_3 - y_2\|} = 0.13795$$
$$\vdots$$

The computed β_i's are less than one that indicates the convergence of MVIM for this test case. Fig. 7 shows a comparison of the solution obtained with VIM and MVIM using four series terms of the truncated series against the exact solution (31). It can be noticed that MVIM coincides with analytic solution for $t = 1$, however, VIM gives the negative value of number density function which limits its application in the dairy sciences. In Table 3, the truncation error between the analytic and the numerical solutions estimated by VIM and MVIM is calculated for $t = 1$ and $p \in [0, 7]$ for the product kernel. As expected, MVIM gives less error over VIM. In other words, the MVIM is a more sophisticated and efficient approach to capture the distribution for larger time domains.

Now, we consider the product kernel for the Eqs. (1)–(2) with an initial iteration $y_0(p) = \frac{e^{-p}}{p}$. Again, from (30), we get the following iterations

$$y_1(p,t) = \mathrm{e}^{-p}\left(\frac{1}{p} + \frac{\mathrm{e}^{-t}\left(\mathrm{e}^{t}-1\right)(p-2)}{2}\right),$$
$$y_2(p,t) = \mathrm{e}^{-p}\left(-1 + \mathrm{e}^{-t} + \frac{p}{2} - \frac{p\mathrm{e}^{-t}}{2} + \frac{1}{p}\right) + \sinh(p+t)\left(\frac{3p}{2} - p^2 + \frac{p^3}{6} + \cosh(t) + \sinh(t) - \frac{3p\cosh(t)}{2} - \frac{3p\sinh(t)}{2} + p^2\cosh(t) - \frac{p^3\cosh(t)}{6} + p^2\sinh(t) - \frac{p^3\sinh(t)}{3} + \frac{p^4\sinh(t)}{12} - \frac{p^5\sinh(t)}{120}\right) + \cosh(p+t)\left(1 - \frac{3p}{2} + p^2 - \frac{p^3}{6} - \cosh(t) - \sinh(t) + \frac{3p\cosh(t)}{2} + \frac{3p\sinh(t)}{2} - p^2\cosh(t) + \frac{p^3\cosh(t)}{6} - p^2\sinh(t) + \frac{p^3\sinh(t)}{3} - \frac{p^4\sinh(t)}{12} + \frac{p^5\sinh(t)}{120}\right) + t\left(\cosh(p+t)\left(1 - \frac{3p}{2} - \frac{p^3}{3} + p^2 + \frac{p^4}{12} - \frac{p^5}{120}\right) + \sinh(p+t)\left(-1 + \frac{3p}{2} - p^2 + \frac{p^3}{3} - \frac{p^4}{12} + \frac{p^5}{120}\right)\right),$$

and so on. The analytic solution for product kernel with initial condition $y_0(p) = \frac{e^{-p}}{p}$ is as follow [50] :

$$y(p,t) = e^{-\tau p}\,\frac{I_1(2p\sqrt{t})}{p^2\sqrt{t}}. \tag{32}$$

Fig. 8 depicts the analytic solution (32) and numerical solution obtained by VIM and MVIM using three series terms of the truncated series at $t = 1.5$ with $y_0 = e^{-p}/p$ for the product kernel. Similar to the previous cases, MVIM again shows better agreement with the exact solution than the existing VIM. To estimate all results using the MVIM, it took only $31\,s$ of CPU time. The truncation error and moments results are quite similar to the previous case, so to avoid repetition, the results are not shown here.

Example 4.6. Consider the bilinear aggregation kernel $l(p, q) = A + B(p+q) + C(pq)$, where A, B, C are constants for the Eqs. (1)–(2) with $y_0(p) = e^{-p}$ and $y_0(p) = 4pe^{-2p}$.

Our goal is to find the solution for non-zero values of A, B, and C. One may recover a product kernel for A = 0, B = 0 and C = 1, a sum kernel for A = 0, B = 1 and C = 0, and a constant kernel by setting A = 1, B = 0 and C = 0 that has been investigated previously. The analytic solution for bilinear kernel does not exist in the literature, therefore the results are verified against finite volume scheme. For the bilinear kernel, the iterative formula for MVIM (12) reduces to

$$y_{k+1}(p,t) = y_k(p,t) - \int_0^t e^{\eta - t}\left[\frac{\partial y_k(p,\eta)}{\partial \eta} - \frac{1}{2}\int_0^p (A + B(p) + C((p-q)q))y_k(p-q,\eta)y_k(q,\eta)dq + \int_0^\infty (A + B(p+q) + C(pq))y_k(p,\eta)y_k(q,\eta)dq\right]d\eta. \tag{33}$$

By using the above relation with exponential initial distribution $y_0(p) = e^{-p}$, we get the following iterations

$$y_1(p,t) = \mathrm{e}^{-p} - \frac{\mathrm{e}^{-p-t}\left(\mathrm{e}^t - 1\right)\left(12A + 12B - 6Ap + 12Bp + 12Cp - 6Bp^2 - Cp^3\right)}{12},$$

$$y_2(p,t) = -\frac{3A^2}{2} - B^2 + \mathrm{e}^{-p}\left(1 + \mathrm{e}^{-t}(A+B) + \frac{(3A^2 - A^3 + 2B^2)}{2}\right) + \frac{A^3\mathrm{e}^{-p-2t}}{2} - t\left(\frac{3A^2}{2} - B - A - A^3 + B^2 + 3AB + \frac{AC}{2} - 2AB^2 - 3A^2B - A^2C - ABC - 4ABC - 2B^3 + p\left(\frac{A}{2} - B - C - \frac{3A^2}{2} - 4AB^2 + A^2B - AC^2 - \frac{A^2C}{2} + \frac{3A^3}{2} + \frac{5BC}{2} + 3B^2 + AB + 2AC\right) + p^2\left(\frac{A^2}{4} - \frac{A^3}{2} - \frac{B^2}{2} - B^3 + C^2 + \frac{B}{2} - \frac{5AB}{2} - AC + 2BC + 4AB^2 + \frac{5A^2B}{2} + A^2C - BC^2 - 3B^2C + ABC\right) + p^3\left(\frac{A^3}{24} - B^2 + 2B^3 + \frac{C}{12} + \frac{5AB}{12} - \frac{5BC}{4} - \frac{AC}{4} + \frac{5AB^2}{6} - A^2B + \frac{AC^2}{4} + \frac{A^2C}{12} + \frac{5B^2C}{3} + \frac{11ABC}{6}\right) + p^4\left(\frac{B^2}{6} - \frac{B^3}{6} - \frac{C^2}{6} + \frac{AC}{16} - \frac{BC}{6} - \frac{7AB^2}{12} + \frac{A^2B}{12} + \frac{AC^2}{6} - \frac{A^2C}{8} + \frac{5BC^2}{12} + \frac{2B^2C}{3} - \frac{ABC}{8}\right) + p^5\left(\frac{C^3}{30} - \frac{B^3}{12} - B^2Cp + \frac{11BC}{240} + \frac{AB^2}{20} - \frac{AC^2}{24} + \frac{A^2C}{80} + \frac{BC^2}{15} - \frac{17B^2C}{120} - \frac{2ABC}{15}\right) + p^6\left(\frac{ABC}{72} - \frac{AC^2}{180} - \frac{11BC^2}{360} - \frac{B^2C}{40} + \frac{C^2}{360} + \frac{B^3}{120}\right) + p^7\left(\frac{B^2C}{315} - \frac{C^3}{630} - \frac{BC^2}{630} + \frac{17AC^2}{20160}\right) + \frac{BC^2p^8}{2880} + \frac{C^3p^9}{90720}\Bigg) + \mathrm{e}^{-p}\Bigg(-A - B - AB^2 + \frac{AC}{2} - \frac{3A^2B}{2} - \frac{A^2C}{2} - \frac{BC^2}{2} + \frac{ABC}{2} + p\left(\frac{A}{2} - B - C + \frac{3A^3}{4} + 3B^2 - B^3 - \frac{3A^2}{2} - 2AB^2 + \frac{A^2B}{2} - \frac{AC^2}{2} - \frac{A^2C}{4} - \frac{B^2C}{2} - 2ABC\right) + p^2\left(\frac{A^2}{4} - \frac{A^3}{4} - \frac{B^2}{2} - \frac{B^3}{2} + C^2 + \frac{B}{2} + \frac{5A^2B}{4} + \frac{A^2C}{2} + \frac{A^2Cp^5}{160} - \frac{3B^2C}{2} - \frac{5AB}{2} - AC + 2BC + \frac{ABC}{2}\right) + p^3\left(\frac{A^3}{48} - B^2 + B^3 + \frac{5AB^2}{12} - \frac{A^2B}{2} + \frac{C}{12} + \frac{AC^2}{8} + \frac{A^2C}{24} + \frac{5B^2C}{6} + \frac{5AB}{12} - \frac{5BC}{4} - \frac{AC}{4} + \frac{11ABC}{12}\right) + p^4\left(-\frac{B^3}{12} - \frac{C^2}{6} - \frac{7AB^2}{24} + \frac{A^2B}{24} + \frac{AC^2}{12} - \frac{A^2C}{16} + \frac{5BC^2}{24} - \frac{BC}{6} + \frac{B^2}{6} + \frac{AC}{16} - \frac{ABC}{16} + \frac{B^2C}{3}\right) + p^5\left(\frac{C^3}{60} - \frac{B^3}{24} + \frac{AB^2}{40} - \frac{AC^2}{48} + \frac{BC^2}{30} - \frac{17B^2C}{240} + \frac{11BC}{240} - \frac{ABC}{15}\right) + p^6\left(\frac{B^3}{240} + \frac{C^2}{360} - \frac{AC^2}{360} - \frac{11BC^2}{720} - \frac{B^2C}{80} + \frac{ABC}{144}\right) + p^7\left(\frac{17AC^2}{40320} - \frac{C^3}{1260} - \frac{BC^2}{1260} + \frac{B^2C}{630}\right) + \frac{BC^2p^8}{5760} - \frac{C^3p^9}{181440}\Bigg) + \mathrm{e}^{-p-t}\Bigg(-3AB - \frac{AC}{2} + p\left(-\frac{A}{2} + B + C + \frac{3A^2}{2} - 3B^2 - AB - 2AC - \frac{5BC}{2}\right) + p^2\left(-\frac{A^2}{4} + \frac{B^2}{2} - C^2 - \frac{B}{2} + \frac{5AB}{2} - 2BC + AC + 2AB^2\right) + p^3\left(B^2 - \frac{C}{12} - \frac{5AB}{12} + \frac{AC}{4} + \frac{5BC}{4}\right) + p^4\left(\frac{C^2}{6} - \frac{B^2}{6} - \frac{AC}{16} + \frac{BC}{6}\right) - \frac{11BCp^5}{240} - \frac{C^2p^6}{360} - \frac{\left(\mathrm{e}^t - 1\right)\left(12A + 12B - 6Ap + 12Bp + 12Cp - 6Bp^2 - Cp^3\right)}{12}\Bigg) + \mathrm{e}^{-p-2t}\Bigg(\frac{ABC}{2} + p\left(-\frac{3A^3}{4} + B^3 + 2AB^2 - \frac{A^2B}{2} + \frac{AC^2}{2} + \frac{A^2C}{4} + \frac{B^2C}{2} + AB + 2AC + \frac{5BC}{2} + 2ABC + AB^2 + \frac{3A^2B}{2} + \frac{A^2C}{2}\right) + p^2\left(\frac{A^3}{4} - \frac{ABC}{2} + \frac{B^3}{2} - 2AB^2 - \frac{5A^2B}{4} - \frac{A^2C}{2} + \frac{BC^2}{2} + \frac{3B^2C}{2}\right) + p^3\left(-\frac{11ABC}{12} - \frac{A^3}{48} - B^3 - \frac{5AB^2}{12} + \frac{A^2B}{2} - \frac{AC^2}{8} - \frac{A^2C}{24} - \frac{5B^2C}{6}\right) + p^4\left(\frac{ABC}{16} + \frac{B^3}{12} + \frac{7AB^2}{24} - \frac{A^2B}{24} - \frac{AC^2}{12} + \frac{A^2C}{16} - \frac{5BC^2}{24} - \frac{B^2C}{3}\right) + p^5\left(\frac{ABC}{15} - \frac{C^3}{60} + \frac{B^3}{24} - \frac{AB^2}{40} + \frac{AC^2}{48} - \frac{A^2C}{160} - \frac{BC^2}{30} + \frac{17B^2C}{240}\right) + p^6\left(\frac{AC^2}{360} - \frac{ABC}{144} - \frac{B^3}{240} + \frac{11BC^2}{720} + \frac{B^2C}{80}\right) + p^7\left(\frac{C^3}{1260} - \frac{17AC^2}{40320} + \frac{BC^2}{1260} - \frac{B^2C}{630}\right) - \frac{BC^2p^8}{5760} - \frac{C^3p^9}{181440}\Bigg).$$

Fig. 9 compares the third iterative term of VIM and MVIM with the FVS solution for the bilinear kernel by taking $A = B = C = 1$ with an exponential initial distribution. For small time period, such as $t = 0.1$, both VIM and MVIM coincide with the FVS solution while for longer time $t = 0.5$, the result predicted by MVIM overlaps with the FVS solution whereas the VIM shows under prediction for the distribution. The MVIM solution for bilinear aggregation kernel with exponential initial condition exactly matches with the FVS solution and took $1695s$ CPU time to estimate these solutions.

Now, we consider the bilinear kernel with gamma initial distribution $y_0(p) = 4pe^{-2p}$. From the iterative formula (33), we get the following iterations

$$y_1(p,t) = 4p\mathrm{e}^{-2p} - \frac{4p\mathrm{e}^{-2p-t}\left(\mathrm{e}^t - 1\right)\left(15A + 15B + 15Bp + 15Cp - 5Ap^2 - Cp^4\right)}{15},$$

$$y_2(p,t) = \mathrm{e}^{-2p}\Bigg(4p - t\mathrm{e}^{-t}\Bigg(-\frac{4AB^2}{3} + p(-4A - 4B + 6A^2 - 4A^3 + 4B^2 - 8AB^2 - 12A^2B - 4A^2C + 12AB + 2AC - 4ABC) + p^2(12B^2 - 8B^3 - 4C - 4B + 10AB + 8AC + 10BC - 20AB^2 - 8A^2B - 4AC^2 - 4A^2C - 4B^2C - 16ABC) + p^3\left(4A^3 - 4A^2 - 5B + 4B^2 - 8B^3 + 4C^2 - 4AB + 8BC + 8A^2B - 4BC^2 - 12B^2C - 4ABC + \frac{4A}{3} - \frac{4AB^2}{3} + \frac{4A^2C}{3}\right) + p^4\left(-4B^2 + \frac{8B^3}{3} + \frac{4B}{3} - \frac{8AC}{3} - \frac{20AB}{3} + \frac{40AB^2}{3} + 8A^2B + \frac{8A^2C}{3}\right)$$

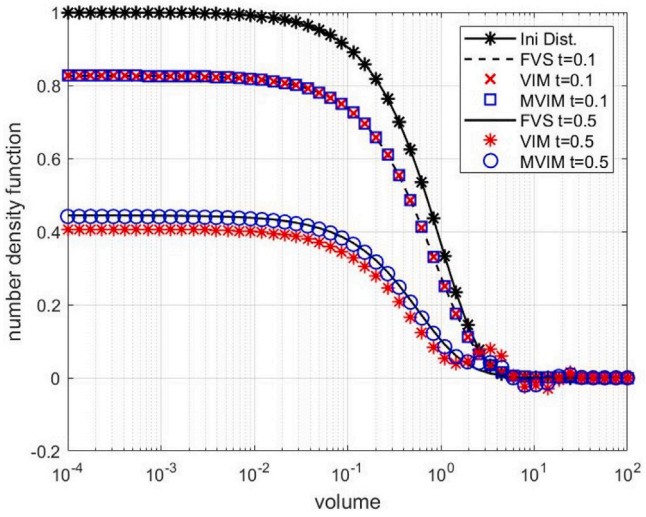

Fig. 9. Testing of VIM, MVIM and FVS solution for bilinear kernel ($A = 1,\ B = 1,\ C = 1$) with $y_0 = e^{-p}$ at time t = 0.1 and t=0.5.

$$+\frac{16ABC}{3}\Big)+p^5\Big(\frac{4A^2}{15}-\frac{8A^3}{15}-\frac{8B^2}{3}+\frac{16B^3}{3}+\frac{4C}{15}-\frac{4AC}{5}-\frac{52BC}{15}+\frac{68AB^2}{15}-\frac{8A^2B}{15}+\frac{4AC^2}{5}+\frac{4A^2C}{5}+\frac{68B^2C}{15}+\frac{16ABC}{3}\Big)+p^6$$
$$\Big(\frac{8B^3}{15}-\frac{8C^2}{15}+\frac{4AB}{9}-\frac{8BC}{15}-\frac{8AB^2}{9}-\frac{16A^2B}{15}+\frac{8AC^2}{15}-\frac{8A^2C}{45}+\frac{4BC^2}{3}+\frac{32B^2C}{15}+\frac{4ABC}{5}\Big)+p^7\Big(\frac{8B^2}{45}-\frac{16B^3}{45}+\frac{4C^3}{35}+\frac{8AC}{105}-$$
$$\frac{40AB^2}{63}-\frac{16A^2C}{105}+\frac{8BC^2}{35}+\frac{4B^2C}{35}-\frac{136ABC}{315}+\frac{4A^3}{315}\Big)+p^8\Big(-\frac{32B^3}{315}+\frac{2BC}{35}+\frac{8A^2B}{315}-\frac{16AC^2}{315}-\frac{68B^2C}{315}-\frac{52ABC}{315}\Big)+p^9\Big(\frac{4C^2}{945}+$$
$$\frac{44AB^2}{2835}-\frac{8AC^2}{945}+\frac{4A^2C}{945}-\frac{8BC^2}{189}-\frac{32B^2C}{945}\Big)+p^{10}\Big(\frac{8B^3}{2835}-\frac{4C^3}{1575}-\frac{4BC^2}{1575}+\frac{68ABC}{14175}\Big)+p^{11}\Big(\frac{52AC^2}{155925}+\frac{188B^2C}{155925}\Big)+\frac{8BC^2p^{12}}{51975}+$$
$$\frac{4C^3p^{13}}{675675}\Big)+e^{-t}\Big(p(4B-6A^2-4B^2+4A-12AB-2AC)+p^2(4B-12B^2+4C-10AB-8AC-10BC)+p^3(4A^2-4B^2-4C^2-\frac{4A}{3}+$$
$$4AB-8BC)+p^4\Big(4B^2-\frac{4B}{3}+\frac{20AB}{3}+\frac{8AC}{3}\Big)+p^5\Big(\frac{8B^2}{3}-\frac{4C}{15}-\frac{4A^2}{15}+\frac{4AC}{5}+\frac{52BC}{15}\Big)+p^6\Big(\frac{8C^2}{15}-\frac{4AB}{9}+\frac{8BC}{15}\Big)-p^7\Big(\frac{8B^2}{45}+$$
$$\frac{8AC}{105}\Big)-\frac{2BCp^8}{35}-\frac{4C^2p^9}{945}+\frac{4p\left(15A+15B+15Bp+15Cp-5Ap^2-5Bp^3-Cp^4\right)}{15}\Big)+\mathrm{e}^{-2t}\Big(p(2A^3+4AB^2+6A^2B+2A^2C+2ABC)$$
$$+p^2(10AB^2+4B^3+4A^2B+2AC^2+2A^2C+2B^2C+8ABC)+p^3\Big(4B^3-2A^3-4A^2B+2ABC+2BC^2+6B^2C+\frac{2AB^2}{3}-\frac{2A^2C}{3}\Big)$$
$$+p^4\Big(-\frac{4B^3}{3}-\frac{20AB^2}{3}-4A^2B-\frac{4A^2C}{3}-\frac{8ABC}{3}\Big)+p^5\Big(\frac{4A^3}{15}-\frac{8B^3}{3}-\frac{34AB^2}{15}+\frac{4A^2B}{15}-\frac{2AC^2}{5}-\frac{2A^2C}{5}-\frac{34B^2C}{15}-\frac{8ABC}{3}\Big)+p^6$$
$$\Big(-\frac{4B^3}{15}+\frac{4AB^2}{9}+\frac{8A^2B}{15}-\frac{4AC^2}{15}+\frac{4A^2C}{45}-\frac{2BC^2}{3}-\frac{16B^2C}{15}-\frac{2ABC}{5}\Big)+p^7\Big(\frac{8B^3}{45}-\frac{2A^3}{315}-\frac{2C^3}{35}+\frac{20AB^2}{63}+\frac{8A^2C}{105}-\frac{4BC^2}{35}-$$
$$\frac{2B^2C}{35}+\frac{68ABC}{315}\Big)+p^8\Big(\frac{16B^3}{315}-\frac{4A^2B}{315}+\frac{8AC^2}{315}+\frac{34B^2C}{315}+\frac{26ABC}{315}\Big)+p^9\Big(\frac{4AC^2}{945}-\frac{2A^2C}{945}-\frac{22AB^2}{2835}+\frac{4BC^2}{189}+\frac{16B^2C}{945}\Big)+p^{10}$$
$$\Big(-\frac{4B^3}{2835}+\frac{2C^3}{1575}+\frac{2BC^2}{1575}-\frac{34ABC}{14175}\Big)+p^{11}\Big(-\frac{26AC^2}{155925}-\frac{94B^2C}{155925}\Big)-\frac{4BC^2p^{12}}{51975}-\frac{2C^3p^{13}}{675675}\Big)+p(-4A-4B+6A^2-2A^3+4B^2+12AB$$
$$+2AC-4AB^2-6A^2B-2ABC)+p^2\Big(12B^2-4B^3-4B-4C-10AB^2-4A^2B-2AC^2-2A^2C-2B^2C+10AB+8AC+10BC-8AB$$
$$C\Big)+p^3\Big(-4A^2+2A^3+4B^2-4B^3+4C^2+\frac{4A}{3}-\frac{2AB^2}{3}+4A^2B+\frac{2A^2C}{3}-2BC^2-6B^2C-4AB+8BC-2ABC\Big)+p^4\Big(-4B^2+\frac{4B^3}{3}+$$
$$\frac{4B}{3}+\frac{20AB^2}{3}+4A^2B+\frac{4A^2C}{3}-\frac{20AB}{3}-\frac{8AC}{3}+\frac{8ABC}{3}\Big)+p^5\Big(\frac{4A^2}{15}-\frac{4A^3}{15}-\frac{8B^2}{3}+\frac{8B^3}{3}+\frac{4C}{15}+\frac{34AB^2}{15}-\frac{4A^2B}{15}+\frac{2AC^2}{5}+\frac{2A^2C}{5}$$
$$+\frac{34B^2C}{15}-\frac{4AC}{5}-\frac{52BC}{15}+\frac{8ABC}{3}\Big)+p^6\Big(\frac{4B^3}{15}-\frac{8C^2}{15}-\frac{4AB^2}{9}-\frac{8A^2B}{15}+\frac{4AC^2}{15}-\frac{4A^2C}{45}+\frac{2BC^2}{3}+\frac{16B^2C}{15}+\frac{4AB}{9}-2A^2Cp-\frac{8BC}{15}$$
$$+\frac{2ABC}{5}\Big)+p^7\Big(\frac{2A^3}{315}+\frac{8B^2}{45}-\frac{8B^3}{45}+\frac{2C^3}{35}-\frac{20AB^2}{63}-\frac{8A^2C}{105}+\frac{4BC^2}{35}+\frac{2B^2C}{35}+\frac{8AC}{105}-\frac{68ABC}{315}\Big)+p^8\Big(-\frac{16B^3}{315}+\frac{4A^2B}{315}-\frac{8AC^2}{315}-$$
$$\frac{34B^2C}{315}+\frac{2BC}{35}-\frac{26ABC}{315}\Big)+p^9\Big(\frac{4C^2}{945}+\frac{22AB^2}{2835}-\frac{4AC^2}{945}+\frac{2A^2C}{945}-\frac{4BC^2}{189}-\frac{16B^2C}{945}\Big)+p^{10}\Big(\frac{4B^3}{2835}-\frac{2C^3}{1575}-\frac{2BC^2}{1575}+\frac{34ABC}{14175}\Big)+$$
$$p^{11}\Big(\frac{26AC^2}{155925}+\frac{94B^2C}{155925}\Big)+\frac{4BC^2p^{12}}{51975}+\frac{2C^3p^{13}}{675675}-\frac{4p\left(15A+15B+15Bp+15Cp-5Ap^2-5Bp^3-Cp^4\right)}{15}\Big).$$

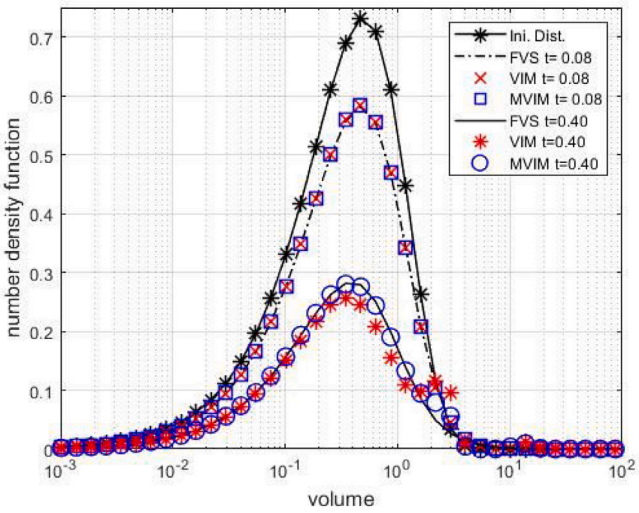

Fig. 10. Testing of VIM, MVIM and FVS for bilinear kernel ($A = B = C = 1$) with $y_0 = 4pe^{-2p}$ at time $t = 0.08$ and $t = 0.40$.

Similar to the previous cases, Fig. 10 shows the comparison of both VIM and MVIM against the finite volume scheme for bilinear kernel corresponding to a gamma initial distribution by taking $A = 1$, $B = 1$, and $C = 1$. The results demonstrate consistent behaviour with previous cases, that is, both VIM and MVIM coincide with the FVS solution for a short time period ($t = 0.08$). However, for a longer time period ($t = 0.40$), the MVIM exhibits superior performance compared to the VIM. MVIM estimate the series solution by consuming $2109s$ CPU time for the bilinear aggregation kernel with gamma initial condition and overlaps with the FVS solution.

5. Concluding remarks and future prospects

We present a modified variational iteration method for obtaining series solutions to the nonlinear aggregation population balance equation. This new approach utilizes fewer terms and addresses the accuracy issues encountered when dealing with longer time domains. The convergence analysis is established, and error estimates are provided to support the validity of the method. To demonstrate the accuracy and applicability of the modified variational iteration method, several numerical examples are worked out. We compute new series solutions for the nonlinear aggregation population balance equation corresponding to polymerization, Ruckenstein/Pulvermacher, and generalized bilinear kernels. As exact solutions for these kernels are not available in the literature, we validate the results of the new approach against the finite volume scheme. The obtained results show that this approach has the tendency to capture the series solution accurately for both analytically tractable (sum, product and bilinear kernels) and physically relevant kernels. It is evident that the modified variational iteration method outperforms the traditional variational iteration method when applied to longer time domains. It has been also shown that the proposed approach approximate the zeroth and first order moments with higher accuracy than the existing approaches by consuming few series terms.

Given the high accuracy and efficiency demonstrated by the modified variational iteration method, we plan to extend its application in the future to track multiple properties of systems governed by multidimensional aggregation and fragmentation population balance equations [58–61].

Ethical approval

Principles of ethics are taken into account to guarantee the highest possible standards in all aspects of research.

CRediT authorship contribution statement

Sonia Yadav: Formal analysis, Investigation, Methodology, Validation, Writing – original draft, Writing – review & editing. **Mehakpreet Singh:** Conceptualization, Formal analysis, Investigation, Methodology, Software, Supervision, Validation, Visualization, Writing – original draft, Writing – review & editing. **Sukhjit Singh:** Formal analysis, Investigation, Supervision, Validation, Visualization, Writing – review & editing. **Stefan Heinrich:** Formal analysis, Supervision, Validation, Visualization, Writing – review & editing. **Jitendra Kumar:** Formal analysis, Investigation, Supervision, Validation, Visualization, Writing – review & editing.

Declaration of competing interest

The authors declare that they have no known competing financial interests or personal relationships that could have appeared to influence the work reported in this paper.

Data availability

No data was used for the research described in the article.

Funding acknowledgement

The authors acknowledge the Alexander von Humboldt Foundation (Grant No. 3.4-1146221-IND-IP) for their support within the framework of the Research Group Linkage Programme.

References

[1] Samsel Richard W, Perelson Alan S. Kinetics of rouleau formation. I. A mass action approach with geometric features. Biophys J 1982;37(2):493–514.
[2] Lissauer Jack J. Planet formation. Ann Rev Astron Astrophys 1993;31(1):129–72.
[3] Ramkrishna Doraiswami. Population balances: Theory and applications to particulate systems in engineering. Elsevier; 2000.
[4] Gunawan Rudiyanto, Fusman Irene, Braatz Richard D. High resolution algorithms for multidimensional population balance equations. AIChE J 2004;50(11):2738–49.
[5] Eggersdorfer Maximilian L, Pratsinis Sotiris E. Agglomerates and aggregates of nanoparticles made in the gas phase. Adv Powder Technol 2014;25(1):71–90.
[6] Hasseine Abdelmalek, Bart Hans Jörg. Adomian decomposition method solution of population balance equations for aggregation, nucleation, growth and breakup processes. Appl Math Model 2015;39(7):1975–84.
[7] Singh Mehakpreet, Singh Randhir, Singh Sukhjit, Singh Gagandeep, Walker Gavin. Finite volume approximation of multidimensional aggregation population balance equation on triangular grid. Math Comput Simulation 2020;172:191–212.
[8] Singh Mehakpreet, Matsoukas Themis, Walker Gavin. Two moments consistent discrete formulation for binary breakage population balance equation and its convergence. Appl Numer Math 2021;166:76–91.
[9] Singh Mehakpreet, Ismail Hamza Y, Matsoukas Themis, Albadarin Ahmad B, Walker Gavin. Mass-based finite volume scheme for aggregation, growth and nucleation population balance equation. Proc R Soc Lond Ser A Math Phys Eng Sci 2019;475(2231):20190552.
[10] Singh Mehakpreet, Matsoukas Themis, Walker Gavin. Mathematical analysis of finite volume preserving scheme for nonlinear Smoluchowski equation. Physica D 2020;402:132221.
[11] Smoluchowski Marian V. Versuch einer mathematischen Theorie der Koagulationskinetik kolloider Lösungen. Z Phys Chem 1918;92(1):129–68.
[12] Leyvraz François. Scaling theory and exactly solved models in the kinetics of irreversible aggregation. Phys Rep 2003;383(2–3):95–212.
[13] Kaur Gurmeet, Singh Randhir, Singh Mehakpreet, Kumar Jitendra, Matsoukas Themis. Analytical approach for solving population balances: a homotopy perturbation method. J Phys A 2019;52(38):385201.
[14] Yadav Nisha, Singh Mehakpreet, Singh Sukhjit, Singh Randir, Kumar Jitendra. A note on homotopy perturbation approach for nonlinear coagulation equation to improve series solutions for longer times. Chaos Solitons Fractals 2023;173:113628.
[15] Kumar Jitendra, Warnecke Gerald. A note on moment preservation of finite volume schemes for solving growth and aggregation population balance equations. SIAM J Sci Comput 2010;32(2):703–13.
[16] Giri Ankit Kumar, Hausenblas Erika. Convergence analysis of sectional methods for solving aggregation population balance equations: The fixed pivot technique. Nonlinear Anal RWA 2013;14(6):2068–90.
[17] Singh Mehakpreet, Ghosh Dhrubajyoti, Kumar Jitendra. A comparative study of different discretizations for solving bivariate aggregation population balance equation. Appl Math Comput 2014;234:434–51.
[18] Singh Mehakpreet, Kumar Jitendra, Bück Andreas, Tsotsas Evangelos. An improved and efficient finite volume scheme for bivariate aggregation population balance equation. J Comput Appl Math 2016;308:83–97.
[19] Nguyen Tan Trung, Laurent Frédérique, Fox Rodney O, Massot Marc. Solution of population balance equations in applications with fine particles: mathematical modeling and numerical schemes. J Comput Phys 2016;325:129–56.
[20] Gelbard Fred M, Seinfeld John H. Coagulation and growth of a multicomponent aerosol. J Colloid Interface Sci 1978;63(3):472–9.
[21] Mostafaei Peyman, Rajabi-Hamane Mehdi. Numerical solution of the population balance equation using an efficiently modified cell average technique. Comput Chem Eng 2017;96:33–41.
[22] Ahrens Robin, Le Borne Sabine. FFT-based evaluation of multivariate aggregation integrals in population balance equations on uniform tensor grids. J Comput Appl Math 2018;338:280–97.
[23] Singh Mehakpreet, Ismail Hamza Y, Singh Randhir, Albadarin Ahmad B, Walker Gavin. Finite volume approximation of nonlinear agglomeration population balance equation on triangular grid. J Aerosol Sci 2019;137:105430.
[24] Singh Mehakpreet, Singh Randhir, Singh Sukhjit, Walker Gavin, Matsoukas Themis. Discrete finite volume approach for multidimensional agglomeration population balance equation on unstructured grid. Powder Technol 2020;376:229–40.
[25] Singh Mehakpreet. Accurate and efficient approximations for generalized population balances incorporating coagulation and fragmentation. J Comput Phys 2021;435:110215.
[26] Wang Kangle. Exact traveling wave solutions for the local fractional Kadomtsov–Petviashvili–Benjamin–Bona–Mahony model by variational perspective. Fractals 2022;30(06):2250101.
[27] Wang Kangle. Novel traveling wave solutions for the fractal Zakharov–Kuznetsov–Benjamin–Bona–Mahony model. Fractals 2022;30(09):2250170.
[28] Wang KangLe, Wei ChunFu. Fractal soliton solutions for the fractal-fractional shallow water wave equation arising in ocean engineering. Alex Eng J 2023;65:859–65.
[29] Wang Kang-Le. New perspective on fractional hamiltonian amplitude equation. Opt Quantum Electron 2023;55(12):1033.
[30] Wang Kang-Le. Investigation of the fractional Kdv–Zakharov–Kuznetsov equation arising in plasma physics. Fractals 2023;55(07):2350065.
[31] Wang Kang Le. Novel approaches to fractional Klein–Gordon–Zakharov equation. Fractals 2023;31(07):2350095.
[32] Wang Kang-Le. Totally new soliton phenomena in the fractional Zoomeron model for shallow water. Fractals 2023;31(03):2350029.
[33] Biazar Jafar, Ayati Zainab, Yaghouti Mohammad Reza. Homotopy perturbation method for homogeneous Smoluchowsk's equation. Numer Methods Partial Differential Equations 2010;26(5):1146–53.
[34] Singh Randhir, Saha Jitraj, Kumar Jitendra. Adomian decomposition method for solving fragmentation and aggregation population balance equations. J Appl Math Comput 2015;48:265–92.
[35] Hasseine Abdelmalek, Attarakih Menwer, Belarbi Rafik, Bart Hans Jörg. On the semi-analytical solution of integro-partial differential equations. Energy Procedia 2017;139:358–66.
[36] Yadav Sonia, Keshav Somveer, Singh Sukhjit, Singh Mehakpreet, Kumar Jitendra. Homotopy analysis method and its convergence analysis for a nonlinear simultaneous aggregation-fragmentation model. Chaos Solitons Fractals 2023;177:114204.
[37] Kaushik Sonali, Kumar Rajesh. A novel optimized decomposition method for Smoluchowski's aggregation equation. J Comput Appl Math 2023;419:114710.
[38] Arora Gourav, Hussain Saddam, Kumar Rajesh. Comparison of variational iteration and Adomian decomposition methods to solve growth, aggregation and aggregation-breakage equations. J Comput Sci 2023;67:101973.
[39] Heydari M, Loghmani GB, Hosseini SM, Yildirim A. A novel hybrid spectral-variational iteration method (HS-VIM) for solving nonlinear equations arising in heat transfer. Iran J Sci Technol Trans A-Sci 2013.
[40] Heydari M, Loghmani GB, Hosseini SM. An improved piecewise variational iteration method for solving strongly nonlinear oscillators. Comput Appl Math 2015;34:215–49.
[41] Heydari Mohammad, Loghmani Ghasem Barid, Wazwaz Abdul-Majid. A numerical approach for a class of astrophysics equations using piecewise spectral-variational iteration method. Internat J Numer Methods Heat Fluid Flow 2017;27(2):358–78.
[42] Soltani L Ahmad, Shirzadi Ahmad. A new modification of the variational iteration method. Comput Math Appl 2010;59(8):2528–35.
[43] He Ji Huan. Variational iteration method–a kind of non-linear analytical technique: some examples. Int J Non-linear Mech 1999;34(4):699–708.
[44] Ali AHA, Raslan KR. Variational iteration method for solving biharmonic equations. Phys Lett A 2007;370(5–6):441–8.
[45] Kafash Behzad, Rafiei Zahra, Karbassi Seyed M, Wazwaz Abdul M. A computational method based on the modification of the variational iteration method for determining the solution of the optimal control problems. Int J Numer Modelling, Electron Netw Devices Fields 2020;33(5):e2739.
[46] Nuseir Ameina S, Al-Towaiq Mohammad. The modified variational iteration method for solving the impenetrable Agar model problem. Int J Pure Appl Math 2014;96(4):445–56.

[47] Noor Muhammad Aslam, Noor Khalida Inayat, Rafiq Muhammad, Al-said Eisa A. Variational iteration method for solving a system of second order boundary value problems. Int J Nonlinear Sci Numer Simul 2010;11(12):1109–20.
[48] Kumar Jitendra, Kaur Gurmeet, Tsotsas Evangelos. An accurate and efficient discrete formulation of aggregation population balance equation. Kinet Relat Models 2016;9(2).
[49] Zidar Mitja, Kuzman Drago, Ravnik Miha. Characterisation of protein aggregation with the Smoluchowski coagulation approach for use in biopharmaceuticals. Soft Matter 2018;14(29):6001–12.
[50] Ranjbar Mojtaba, Adibi Hojatollah, Lakestani Mehrdad. Numerical solution of homogeneous Smoluchowski's coagulation equation. Int J Comput Math 2010;87(9):2113–22.
[51] Liu Anxiong, Rigopoulos Stelios. A conservative method for numerical solution of the population balance equation, and application to soot formation. Combust Flame 2019;205:506–21.
[52] Scott William T. Analytic studies of cloud droplet coalescence I. J Atmospheric Sci 1968;25(1):54–65.
[53] Aldous David J. Deterministic and stochastic models for coalescence (aggregation and coagulation): a review of the mean-field theory for probabilists. Bernoulli 1999;3–48.
[54] Ruckenstein Eli, Pulvermacher B. Growth kinetics and the size distributions of supported metal crystallites. J Catalysis 1973;29(2):224–45.
[55] McMahon Donald J, Brown Rodney J. Enzymic coagulation of casein micelles: a review. J Dairy Sci 1984;67(5):919–29.
[56] Ernst Matthieu H, Ziff Robert M, Hendriks Eric. Coagulation processes with a phase transition. J Colloid Interface Sci 1984;97(1):266–77.
[57] Odibat Zaid M. A study on the convergence of variational iteration method. Math Comput Modelling 2010;51(9–10):1181–92.
[58] Singh Mehakpreet, Vuik Kees, Kaur Gurmeet, Bart Hans-Jörg. Effect of different discretizations on the numerical solution of 2D aggregation population balance equation. Powder Technol 2019;342:972–84.
[59] Singh Mehakpreet, Kumar Ashish, Shirazian Saeed, Ranade Vivek, Walker Gavin. Characterization of simultaneous evolution of size and composition distributions using generalized aggregation population balance equation. Pharmaceutics 2020;12(12):1152.
[60] Singh Mehakpreet. New finite volume approach for multidimensional Smoluchowski equation on nonuniform grids. Stud Appl Math 2021;147(3):955–77.
[61] Singh Mehakpreet, Matsoukas Themis, Ranade Vivek, Walker Gavin. Discrete finite volume formulation for multidimensional fragmentation equation and its convergence analysis. J Comput Phys 2022;464:111368.